We appreciate the time and constructive comments from anonymous reviewers and the editor on our manuscript. A point-by-point summary of the modifications that we have declared to make before in response to the reviewers' comments are included below. The reviewers' comments are indicated in italic font and our responses are in regular font.

Reviewer #1

Reviewer:

These are my comments of the work entitled: An improved parameterization of leaf area index (LAI) seasonality in the Canadian Land Surface Scheme (CLASS) and Canadian Terrestrial Ecosystem Model (CTEM) modelling framework. Firstly, I want to thank the authors for the work done. I felt the manuscript quite interesting. This paper describes the addition of the Non Structural Carbohydrates (NSC) module, to the CLASS-CTEM model. NSC module allows to better represent Leaf Area seasonality, as well as to provide a mobile carbohydrate pool to the trees to increase its resilience to disturbances in absence of photosynthesis. It is tested in three Fluxnet sites, where GPP, LAI, and heat fluxes (Incident radiation, latent heat and sensible heat) model projections are contrasted against real data. In my opinion, this is an interesting, thoroughfull work, where the authors clearly demonstrate that the addition of the NSC module clearly improves model performance. My major concerns about the present paper are about its novelty. Currently most of process-based forest simulation models does include the NSC module (Fontes et al., 2010), in a similar way than the new module for the CLASS-CTEM model. So, in my opinion, your current manuscript doesn't clarify the novelty of your work. Furthermore, throughout your manuscript there is little reference to other models that include this key compartment, and I think it would be a nice element to include in the discussion, as there is plenty of other works in which the addition of NSC in a given model clearly improves its performance.

Authors:

References to existing work on inclusion of NSC pools in ecosystem models have been added to the manuscript (lines 102-121). Although NSC pools have been included in other process-based models, the CLASS-CTEM model lacked this part and the present study is the first effort to address this problem. While we do not claim novelty for the present study, we have clarified and stressed the importance of NSC pools even more in the revised version of our manuscript (lines 222-227, 453-456, 571-577, 608-612, 619-629).

Reviewer:

Specific considerations:

I felt a little lacking how the Maintenance respiration was calculated in CLASS-CTEM. I've seen other reviewers asking for the same point, and I feel like an addition of the maintenance respiration formula as well as the assumptions of the model about this process would improve significantly the paper. Besides, I have a couple of questions about maintenance respiration: it is dependent on temperature? It is assumed the same respiration rate for the structural and non-structural carbohydrates?

In lines 175-177, you state that respiratory carbon loses are assumed to occur from the non-structural

part. Does it mean that structural carbon is not accounted in maintenance respiration? I guess you did not mean that, but as it is stated, it may lead to misinterpretations.

Authors:

The text was modified and some clarifications were added in response to the editor's review (lines 178-185 and 216-218) in the context of maintenance respiration. The model's maintenance respiration along with other processes have already been discussed in previous publications (e.g., section A3.1 in Melton and Arora, 2016).

Yes, indeed maintenance respiration is temperature dependent. In the modified (i.e., NSC-added) version of the model presented in this study, maintenance respiration occurs only from the non-structural pools consistent with observational and modelling studies (e.g., Hoch et al., 2003; Sperling et al., 2015; and Li et al., 2016) which show that plants' NSC stores become depleted during dormant season and cold and drought stresses due to excess respiration (lines 196-199).

Reviewer:

It is a minor issue, but, in general, I think your explanations about Leaf Area (LA) importance upon photosynthesis. However, I think you are wrong when referring to them as LAI (for example, lines 1, 63). LAI doesn't perform photosynthesis, it is the Leaf Area, that does it. LAI is just an explanatory index about the surface of leaf area per unit of surface.

Authors:

We feel this is a terminology issue. While it is true that photosynthesis is a function of the total "leaf area", several of the model's parameterizations use leaf area index since all model processes are simulated per unit area. For example, CLASS-CTEM model uses the Beer-Lambert law ($1-e^{-k(LAI)}$, where k is a vegetation-dependent light extinction coefficient) to scale photosynthesis from the leaf to the canopy level. The related text has been modified (lines 176-177) to reflect this.

Reviewer:

In point 2.1.1 (Reallocation of non-structural carbon during leaf out period), you do state that "after reaching a threshold LAI, NPP is allocated to stem and roots in addition to leaves". I could not find in your work how these compartments are developed. Do your model follow any predefined rule (e.g. the Pipe model rule, Shinozaky, 1974)? Or they are equally allocated throughout the tree compartments according to a predefined rate?

Line 451. Again, following which rule, besides the "after reaching a LAI threshold", are the carbohydrates allocated through the three compartments? A fixed rate? A mechanistic rule?

Authors:

While the model's several processes have been described before in Melton and Arora (2016), additional details are added at lines 276-285 to clarify these allocation-related questions raised by the reviewer. In brief, the model uses dynamically calculated allocation fractions for leaves, stems and

roots based on light, water and leaf phenological status of vegetation. The preferential allocation of carbon to the different tissue pools is based on three assumptions: (i) if soil moisture is limiting, carbon should be preferentially allocated to roots for greater access to water, (ii) if LAI is low, carbon should be allocated to leaves for enhanced photosynthesis and finally (iii) carbon is allocated to the stem to increase vegetation height and lateral spread of vegetation when the increase in LAI results in a decrease in light penetration. The dynamically calculated allocation fractions are further modified to ensure that root to shoot ratio is realistic and that there is enough woody biomass to support green biomass.

Reviewer:
Line 372-373. I would remove the sentence "The figure legends, in addition to identifying the two mode versions and observations, also show the mean annual value of the quantity plotted", and I would include it in the figure footnote.

Authors:
Agreed.

Reviewer:
Lines 419-420. Your sentence assumes an equilibrium between the atmospheric CO_2 and the biosphere. Maybe is far beyond the discussion of your paper, but I think that this is not strictly true, as there has been previous works identifying the instability of the atmosphere-biosphere complex (e.g. Higgins et al., 2002). It is a minor change, but I would suggest to erase the "currently" in the sentence, thus indicating the responsive nature of biosphere to historical changes in atmospheric CO_2.

Authors:
Agreed.

Reviewer:
Point 3.3. Here, you find that you do overestimate latent heat when modelling your three forests. Are there any research papers about evapotranspiration experiments in those forests? If they are, maybe you should transform latent heat into evapotranspiration values, so you can compare them to your data, and you might then have a better explanation about why does your model overestimates so high the evapotranspiration (Latent heat). In addition, how do this relate to your overestimation of Leaf Area? I see a little discussion about it in lines 508-512, but I think you minimize the effect that you overestimate the LAI during the growing season by about 2 m^2/m^2 in each plot, and this affect both the evapotranspiration at canopy level, but also to the evaporative energy available at ground level.

Authors:
As the reviewer noted evapotranspiration and latent heat fluxes are the same quantity but in different units. Evapotranspiration is expressed in water units (mm) and latent heat flux is expressed in energy

units (W/m^2). At the flux net sites latent heat flux is available but as mentioned in section 3.3 of the manuscript it suffers from energy balance closure. So it is difficult to conclusively determine how much of this overestimation is due to overestimation by the model and how much of it is due to bias in the observed data. Our experience with the CLASS-CTEM model in the past has been that in locations where soil moisture constraint is not very large, as is the case at these three sites, total evapotranspiration is controlled by available energy. Hence the expected seasonality in latent heat flux is characterized by higher values during summer and lower during winter at these sites. Since the latent heat flux at these three sites is primarily controlled by available energy the resulting implication is that if evaporative demand cannot be met by transpiration then it will be met by evaporation from the soil. As a result, changes in LAI do not significantly affect total evapotranspiration (or latent heat flux) but change the partitioning of evapotranspiration flux coming from transpiration, evaporation of intercepted water on canopy leaves, and evaporation from the soil. Therefore, had the model simulated lower LAI than it currently does, then the latent heat flux would not have been significantly different from its current values. Additional discussion to make this point has been added (lines 533-543, 587-599).

Reviewer:

Lines 519 to 523. Please, revise the Vmax concept: as states the original paper from Kattge et al, (2009), Vmax is the maximum carboxilation capacity, not the maximum photosynthetic rate. In addition: you are justifying a tautology: This is the parameter that we want to apply to Vmax, so we adjust all other model parameters to fit the results according to this Vmax value. In addition, you finish the sentence with "it is possible that the average Vmax value derived by Kattge et al. (2009) is not representative of [...]". I agree that mean Vmax value not representing correctly your forest performance is a possible explanation, but I would rather discuss that Vmax is not the only constrain to photosynthesis, as Jmax is also limiting assimilation rate.

Authors:

Yes, indeed Vmax is the maximum carboxilation capacity. Thank you for catching this. The text has been modified (line 585). The CLASS-CTEM model uses the Farquhar approach for modelling photosynthesis, and therefore photosynthesis is limited by carboxilation capacity but also light and transport capacity limited rates. However, Vmax remains a very strong parameter that controls photosynthesis in the model. We have clarified this aspect in revising our manuscript (lines 584-599, 608-612).

We did not adjust other model parameters to accommodate Kattge et al. (2009) Vmax values. In fact, the very first version of the model used a value of Vmax of 65 umol CO_2/m^2s for its broadleaf cold deciduous PFT which is close to the value of 57 umol CO_2/m^2s suggested by Kattge et al. (2009).

It is probably worth mentioning that at the global scale the performance of CLASS-CTEM model when implemented in the Canadian Earth System Model (CanESM2) is fairly realistic. Figure 11 of Anav et al. (2013), who compared different Earth system models used in the phase 5 of the coupled model intercomparison project (CMIP5), shows that the CLASS-CTEM's simulated "annual global mean" LAI is among one of the best estimates compared to other models. Figure 9 of Anav et al. (2013) shows

that the model also does a good job in simulating global annual GPP.

Reviewer:

Figures 4-6. I would expand a little the footnote, to include the information that results are represented as averaged daily values. In addition, I would consider to change the Leaf Area Index inner pannel to represent the median values during the vegetative period rather than average values, as I think they would be more indicative of the similarities-differences between Fluxnet measurements and model outputs.

Authors:

Thank you for pointing this out. The figures' footnotes are modified.

Reviewer #2

Reviewer:

General Comments

The study by Asaadi et al. aims to improve the seasonal timing of LAI simulated by the CTEM model by including a representation of non-structural carbon (NSC) pools and fluxes in the model (in addition to a few other modifications). The new developments in the model are tested at three temperate broadleaved deciduous sites against LAI, carbon and energy flux observations. They show an improvement in the timing of various stages in the phenological cycle, and corresponding improvement in the timing of carbon fluxes (though limited improvement in energy fluxes).

This is of use to the land surface modeling community as not all LSMs currently include specific NSC pools and related processes. As the authors have discussed, NSC processes are relevant for other components of biogeochemical cycling or ecosystem functioning, in addition to phenology that they focus on in this study (though this discussion could be expanded).

The paper is clearly written and structured (although the goals of their model development work might be better stated as questions or hypotheses). However, I have some concerns about the lack of breadth of the study and depth of the analyses undertaken, which are detailed more in specific comments and outlined briefly here.

1) The addition of non-structural carbon pools and associated fluxes is the primary focus of the study; however, there are no observations of NSCs used to evaluate the authors' modifications to the model. I would have expected that any model modification would be tested against observations that are directly relevant to the new processes added in the model even though I appreciate that NSC data are scarce (see Dietze et al., 2014 for a review of previous such studies in the literature). Why was this not the case? Although the authors state the sites chosen were those with available LAI data, was it not possible to evaluate this model at any site that had observations of non-structural carbon pools (even if those data came from sites that did not also have LAI data)? The authors only chose three sites representing only one plant functional type. I would think there are a greater number of sites with LAI data that this model could be tested against.

Authors:

As mentioned in many other studies as well as in Dietz et al. (2014), plants physiological processes are extraordinary complex and there is still a considerable debate and lack of understanding regarding the behavior of NSC reserves. In addition, there are huge differences between plant species as to how they use their NSC reserves (e.g., Li et al., 2016; Wiley and Helliker, 2012; and Hoch et al., 2003). We are not aware of any long-term NSC measurements where meteorological data are available to drive the model with and LAI measurements are also available to evaluate the model. The relative size of the NSC pools (~5-10% of the total carbon pool in each component of a tree) is inferred from observations (e.g., Li et al., 2016) and the model aims to achieve this. The NSC-reallocation process during bud burst follows the classic source-sink paradigm. This study is the first attempt to include NSC pools and their associated processes in the CLASS-CTEM model and in our humble opinion model evaluation at three sites is enough to illustrate the proof of the concept. Evaluation of the model at regional and global scales will follow in due course but these are subjects of our future studies.

We have, however, followed on other recommendations of reviewer #2 as explained below in answers to his/her comments.

Reviewer:

2) While the authors detail improvements in their modified model in comparison with observations (though less so for energy fluxes), it is not clear which of the model modifications made (detailed in Sections 2.1.1 to 2.1.4) are responsible for the improvements in the simulated carbon and energy fluxes. The authors could show the impact of each modification individually, before evaluating all together. I think the modeling community would appreciate knowing how each of the different modifications made to the model contributed to the overall improvement in the model. Such an analysis would help them ascertain if there are potential structural deficiencies in their own model, thus placing this work in a wider context.

Authors:

Thank you for this suggestion. We have carried out such an analysis and this is illustrated for the Harvard Forest site in the supplementary information. A similar behavior was seen at the other two sites.

Reviewer:

3) The analysis lacks depth – namely, there is a lack of a rigorous quantitative evaluation of the modified model. It would be useful to include certain metrics to quantify the improvements simulated by the modified model (simple correlations for example). In addition, given the authors state that their primary goal is to address the issue of delayed leaf phenology, their analyses should be focused only on that question; general discussions of model behavior and magnitude of fluxes are distracting, especially given they have decided not to run a historical or transient simulation of the model after the

spinup, with increasing CO_2 and climate.

Authors:

The coefficient of determination (R^2) and root-mean-squared error (RMSE) have been added to Figs. 4, 5, 6, and 10 in the revised version of the manuscript. We, however, respectfully disagree that general discussion of carbon fluxes is distracting. Lines 596-599 justify the inclusion of carbon fluxes.

The rationale for not performing historical transient simulations is discussed in lines 390-400 and 565-570. The conclusions derived in the manuscript will not change even if we were able to perform transient historical simulations. Performing transient historical simulations would have provided the current observation-based annual positive values of net biome productivity to evaluate the model against but this is not the focus of our manuscript.

Reviewer:

4) The authors state in the discussion around lines 534-535 that the omission of NSC pools in the original model was a structural error. However, they do not definitively provide evidence to support their claim that the omission of NSC pools was a structural error. While their results show that this process can improve model LAI temporal dynamics, they have not conclusively shown that this is the only process that could be responsible for any discrepancies between the model and the observations, and therefore how important it is to add these specific processes. Incorporation of NSC pools and fluxes may not be the only process that can alleviate the problems in the simulated LAI. As they go on to state, biological systems are complex and difficult to represent with physical equations in models. To ensure that we do have the right model behavior, the processes we include must be rigorously tested against data corresponding to that process. Ideally, the authors would test alternative functions available in the literature for the processes they have implemented, in order to estimate the structural uncertainty associated with the new model developments. A Bayesian model selection framework could be used in order to select the most parsimonious model based on a model selection criterion (such as the Akaike Information Criterion – see Melaas et al., 2013 for an example). I would also be interested to see an analysis on the uncertainty related the parameters they have implemented. It might then be useful to discuss other NSC related processes that remain poorly understood that are not captured by their new model.

Authors:

An aspect of model testing that we omitted in the manuscript is that in the past we tried implementation of time-dependent maximum carboxylation capacity of Rubisco ($V_{c,max}$) as a function of the day length at each latitude. Since $V_{c,max}$ is typically much larger early on in the growing season than during the latter half of the season, we suspected this may fix the problem of delayed leaf out, but it did not. The fact that plants do indeed use their NSC pools for flushing new leaves and that such parameterizations did not help, indicates that omission of NSC pools in the original model version was indeed a structural error. Testing alternative available parameterizations is a big exercise which is beyond the scope of our study and parameterizations from other models require that they fit within the conceptual framework of

our model.

Reviewer:
5) The discussion lacks depth as to how the models they have implemented compare to other studies that have already implemented NSC models, as well as a discussion of any caveats to their modeling work related to the points I mention here. See specific comments.

Authors:
Thank you for pointing this limitation which was also raised by the other reviewer. We have modified our manuscript to include references to existing works which have included NSC pools in ecosystem models (lines 102-121).

Reviewer:
Specific Comments
Introduction
Lines 109-111: Unless I have misunderstood, this model has been used in a phenology comparison at these sites (Richardson et al., 2012). If I have the right model, it seems to me that the problems in the behavior of CTEM (for simulating LAI) shown in Richardson et al. are different to that in Anav. This shows that there might be other issues in the phenology models already implemented in CTEM due to differences between versions/parameterizations, without the addition of new processes/modifications to the model?

Authors:
Results presented in Richardson et al. (2012) were produced using a very old version (which dates back to year 2005) of the model utilized by a university collaborator who coupled it with his own nitrogen module. The model has evolved considerably since then and includes several new parameterizations. As an example, the two simulated LAIs for the US-UMB site (Fig. 1 in Richardon et al. and Fig. 6 panel a in our study) are not similar.

Reviewer:
Model, data and methods
Sections 2.1.1 and 2.1.2 There is a lack of references and/or reasoning for some of the mechanisms they are implementing in the models and the various assumptions they make in doing so (e.g. assumption that respiratory losses occur from non-structural part – line 176, and the references/reasoning behind formulation in equations 5, 6).
In addition, the reasoning behind fixing certain parameter values needs to be detailed (e.g. why $\mu_i = 70$ *line 191; beta in line 241). Were the parameter values found from the literature, or perhaps they were calibrated based on sensitivity studies or optimization experiments?*

Authors:
Thank you for pointing this out. The related text has been modified and more references and justifications have been added (lines 196-197, 213-221, 230-232, 306-310). For example, maintenance respiration which is temperature dependent occurs only from the nonstructural pools in agreement with observational and modelling studies (e.g., Hoch et al., 2003; Sperling et al., 2015; and Li et al., 2016) which show that plants' NSC stores become depleted due to excess respiration during dormant season and during disturbances such as cold and drought stresses. Since biological processes have to be parameterized their parameters have to be calibrated to obtain realistic model behaviour.

Reviewer:
Line 186: maybe refer to Section 2.1.2 for how is Tj calculated?

Authors:
Agreed.

Reviewer:
Section 2.1.3 Are you referring to the fact that CLASS-CTEM has a flat peak of around 2 months in Anav et al., 2013 Fig 11, as opposed to the sharper (~1 month) peak seen in the observations and other models? In that case, it might be good to just state this in parentheses, as I was distracted by the fact that LAI simulated by CLASS-CTEM does not start to decline until long after the summer solstice (Anav et al., 2013 Fig 11) and much later than the observations. In any case, is there evidence in the literature that allocation fractions is modulated by day length – as represented in Section 2.1.3? No references are given to support the addition of this process. Could this slower rate of decline be due to incorrect parameters/processes related to senescence? Initially I was more distracted by the fact the seasonal cycle is delayed (out of phase) by a month or so. I am not therefore convinced if this correction factor based on day length presented in Section 2.1.3 is needed on top of other structural changes in the model.

Authors:
Yes, indeed there are two problems with simulated global mean LAI – it peaks later on with a much flatter peak, and it starts to increase later than observation-based LAI.
We have modified the related text to clarify this (lines 288-291). Also, additional references have been cited in support of using summer solstice as a date to adjust our allocation fractions (lines 306-310).
In earlier versions of the CLASS-CTEM model, continuous allocation of net primary productivity to leaves led to increase in LAI throughout the growing season rather than a constant or slowly decreasing LAI over the growing season. The effect of the adjustment which we have made to the allocation fraction to leaves after summer solstice is more obvious in the supplementary information which highlights the effect of each model parameterization when implemented incrementally.

Reviewer:

Section 2.1.4 Similarly to Sections 2.1.1 (above), why is a value of 12°C now used for Tleaf_cold? Is this based on the literature, or experiments, or a calibration exercise? Please give details and/or references as to how this value was chosen.

Authors:

The value for T_{cold}^{leaf} has been obtained based on a calibration exercise during our third modification step (section 2.1.4) and its individual effect is shown in supplementary information provided. Model parameters depend on their parameterizations. In the CLASS-CTEM model, leaf loss due to cold stress begins when air temperature falls below the T_{cold}^{leaf} threshold but its rate accelerates as temperature continues to drop. Leaf loss rate due to cold stress is maximum when temperature falls 5 °C below the T_{cold}^{leaf} threshold.

Reviewer:

Section 2.2.2 Please could you detail where you got the site meteorological data from, and which method and/or software you used to gap-fill the met data? Also, please could you detail why you chose to use a CO_2 concentration of 350 ppm (this is detailed around line 418 in the results, but needs to be put here). Finally, please could you detail how the LAI measurements were made at each site? Are there differences between sites? This information would be helpful for readers.

Authors:

As mentioned on lines 384-386 of the discussion manuscript, gap-filled meteorological data are obtained from the Fluxnet network. The part detailing the CO_2 concentration has been moved to section 2.2.2 (lines 390-400). LAI measurements are taken using an LAI-2000 plant canopy analyzer instrument (lines 347-350).

Reviewer:

Results

Figures 4-6: It would be good to state that both simulated and observed values represent averaged daily values across all years where data are present in the figure captions.

Authors:

Agreed. The figure captions have been modified.

Reviewer:

Section 3.1 It would be helpful to have some metrics that show improvement (or lack thereof) between model versions for the full timeseries at each site. Even just RMSE or R would be helpful to quantify this and help put the results in context. This could be added to Table 3 for example.

Authors:

The coefficient of determination (R^2) and root-mean-squared error (RMSE) have been added to Figs. 4, 5, 6, and 10.

Reviewer:
Lines 382-384. It would be helpful if the authors showed a comparison of the observations and the model for each of the different modifications to the model that the authors have made in this study (as described in Sections 2.1.1-2.1.4), in addition to the overall improvement brought about by all modifications together. That way, other modeling groups can assess which modifications might be necessary for their own model – thus making the study useful in a wider context. These may only be put supplementary figures or tables, but it would still be useful to discuss in the text.

Authors:
As mentioned above, we have performed such an analysis and included it in the supplementary information.

Reviewer:
Lines 390-391: This is true, and a good result. However, I also noted there seems to be an offset in the start of LAI and GPP in the observations at both US-MMS and US-UMB. At US-MMS the onset of LAI now better matches the observations, but there is now a bias towards a too early rise in GPP. Similarly, although the LAI at US-UMB now better matches the observations, and the GPP matches the observations very well, there is a still this offset. Why do you think that is? Is there a discrepancy between the two types of observations?

Authors:
Indeed! The observations of GPP and LAI are not perfectly consistent with each other. The two sets of observations are made by different groups of people. This highlights the issue that when comparing model results with observations care must be taken to ensure that observations make sense. This aspect is now discussed in lines 442-452.

Reviewer:
Lines 396-414: Why haven't the authors run a historical simulation after their spinup using increasing CO_2 values, so that they can compare to the observed NEE and ecosystem respiration more directly, rather than comparing the (naturally offset/biased) equilibrium state of the model? I appreciate that the lack of a site and disturbance history would result in biases in the model simulations, but this spinup + historical simulation protocol is very common, and I presume is normally used to run CTEM for model inter-comparisons as well as climate change simulations? The authors state that their primary objective is to evaluate the temporal dynamics. But I do not see any issue therefore with running a historical run – as is the often used protocol – and then stating more clearly that their only goal is to look at the temporal dynamics. In any case, the decision to only compare the model at its equilibrium state (as detailed in lines 421-425 for example) should be put in the methods, not in the

results, so the reader is fully aware before they get to the results.

Authors:

Doing a transient historical simulation for each site requires CO_2 concentration data (which we have) as well as meteorological data (which we do not have). While we mentioned this in our original manuscript we have now expanded on it even more (lines 390-400 and 565-570) . Note that the increased ecosystem respiration at present day is not only due to increased GPP (associated with increasing CO_2) and therefore somewhat increased size of carbon pools (compared to what would be obtained from spinning a model at 350 ppm CO_2), but also the increased temperatures that ecosystems are subjected to over the historical period. Without meteorological data that shows a warming trend over the historical period, we would not be able to properly simulate increased respiration at present day. We perform transient historical simulations on a routine basis but chose not to do so for this study since our objective was to evaluate seasonal dynamics of LAI in a clean manner.

Reviewer:

Section 3.2 Line 440: I am a bit confused as the stem's NSC pool does not get depleted in Figs 7-9c? It decreases a little, but not by a large amount as a fraction of its size? I also would expect that given the addition of NSC pools is the main focus of this study, the model should be evaluated at sites which do have NSC data.

Authors:

Very little carbon is actually needed to construct leaves. In fact, on average, the total NSC pool for trees are estimated to be enough to completely rebuild the whole leaf canopy 1-4 times (Dietze et al., 2014). Even higher values have been mentioned in other studies (e.g., Hoch et al., 2003, and Mei et al., 2015).

Reviewer:

Section 3.3 I find this section somewhat distracting given, aside from the last sentence, the differences between the original and modified model are not discussed much. In fact, the differences are very small. The authors note this, but do not provide any discussion as to why the change in seasonality of the simulated LAI does not alter energy fluxes more, as one might expect.

Authors:

This point has been discussed briefly before in the Discussion section but we have added additional text in section 3.3 as well (lines 533-543). The reason for much lower effect of changes in LAI on latent heat fluxes (or equivalently evapotranspiration), than for GPP, is that while GPP is solely determined by LAI, evaporation also occurs from soil and from intercepted water on canopy leaves. If evaporative demand for a given available energy cannot be met by transpiration then the demand is met by evaporation from soil. Although, of course, soil evaporation also depends on soil moisture in the top soil layer. But generally speaking, the different components of evapotranspirative flux are able to

compensate for each other. As a result, small changes in LAI do not affect latent heat flux as much as they do GPP.

Reviewer:

Discussion and conclusions

Aside from the conclusions part to this section, I find the rest of this section lacks a more in-depth discussion in places. There is some discussion of future perspectives to further improve the modeling of LAI (lines 513-525), and the possibility to include the other processes such as drought mortality and the N cycle due to the requirement to model N in leaf NSC pools (lines 552-554). However, there could also be more discussion of the results that might place them in a wider context. E.g. what are the implications for the wider modeling community? How do your results compare to ways NSC-related processes have been implemented in other NSC modeling studies (see review and references in Dietze et al., 2014). A discussion of any caveats to their work would also be useful. These might include some of the points I raised in my general comments, or a discussion about the uncertainty in NSC processes implemented and/or those that remain poorly understood (as the authors stated in the introduction).

Authors:

More discussion along the lines suggested by the reviewer, including comparison to other models which have implemented NSC pools, has been added to the text (lines 102-121). We have also mentioned some of our failed approaches taken to fix the problem of delayed phenology (lines 608-612).

References:

Anav, A., and Coauthors, 2013: Evaluating the land and ocean components of the global carbon cycle in the CMIP5 earth system models. *J. Climate*, **26**, 6801–6843.

Dietze, M. C., A. Sala, M. S. Carbone, C. I. Czimczik, J. A. Mantooth, A. D. Richardson, and R. Vargas, 2014: Nonstructural carbon in woody plants. *Annual review of plant biology,* **65,** 667-687.

Hoch, G., A. Richter, C. Körner, 2003: Non-structural carbon compounds in temperate forest trees. *Plant Cell Environ.,* **26,** 1067–1081.

Kattge, J., W. Knorr, T. Raddatz, and C. Wirth, 2009: Quantifying photosynthetic capacity and its relationship to leaf nitrogen content for global-scale terrestrial biosphere models. *Global Change Biology,* **15,** 976–991.

Li, N., N. He, G. Yu, Q. Wang, J. Sun, 2016: Leaf non-structural carbohydrates regulated by plant functional groups and climate: evidences from a tropical to cold-temperate forest transect. *Ecological Indicators,* **62,** 22–31.

Mei, L., Y. Xiong, J. Gu, Z. Wang, D. Guo, 2015: Whole-tree dynamics of non-structural carbohydrate and nitrogen pools across different seasons and in response to girdling in two temperate trees. *Oecologia,* **177,** 333–344.

Melton, J. R., V. K. Arora, 2016: Competition between plant functional types in the Canadian Terrestrial Ecosystem Model (CTEM) v. 2.0, *Geosci. Model Dev.,* **9,** 323–361.

Richardson, A. D., R. S. Anderson, M. A. Arain, A. G. Barr, G. Bohrer, G. Chen, J. M. Chen, P. Ciais, K. J. Davis, A. R. Desai, and M. C. Dietze, 2012: Terrestrial biosphere models need better representation of vegetation phenology: results from the North American Carbon Program Site Synthesis. *Global Change Biology,* **18(2),** 566-584.

Sperling, O., J. M. Earles, F. Secchi, J. Godfrey, M. A. Zwieniecki, 2015: Frost induces respiration and accelerates carbon depletion in trees. *PLoS One,* 10:e0144124.

Wiley, E., and B. Helliker, 2012: A re-evaluation of carbon storage in trees lends greater support for carbon limitation to growth. *New Phytologist Trus,* **195,** 285-289.

An improved parameterization of leaf area index (LAI) seasonality in the Canadian Land Surface Scheme (CLASS) and Canadian Terrestrial Ecosystem Model (CTEM) modelling framework

[1]Ali Asaadi, [1]Vivek K. Arora, [2]Joe R. Melton, and [2]Paul Bartlett

[1]Canadian Centre for Climate Modelling and Analysis, Environment and Climate Change Canada

[2]Climate Research Division, Environment and Climate Change Canada

Corresponding author: Ali Asaadi, Canadian Centre for Climate Modelling and Analysis, Victoria, BC, V8W 2Y2, Canada

Email: ali.asaadi@canada.ca

Abstract

Leaf area index (LAI) and its seasonal dynamics are key determinants of vegetation productivity in nature and as represented in terrestrial biosphere models seeking to understand land-surface atmosphere flux dynamics and its response to climate change. Non-structural carbohydrates (NSCs) and their seasonal variability are known to play a crucial role in seasonal variation of leaf phenology and growth and functioning of plants. The carbon stored in NSC pools provides a buffer during times when supply and demand of carbon are asynchronous. An example of this role is illustrated when NSCs from previous years are used to initiate leaf onset at the arrival of favourable weather conditions. In this study, we incorporate NSC pools and associated parameterizations of new processes in the modelling framework of the Canadian Land Surface Scheme-Canadian Terrestrial Ecosystem Model (CLASS-CTEM) with an aim to improve the seasonality of simulated LAI. The performance of these new parameterizations is evaluated by comparing simulated LAI and atmosphere-land CO_2 fluxes, to their observation-based estimates, at three sites characterized by broadleaf cold deciduous trees selected from the Fluxnet database. Results show an improvement in leaf onset and offset times with about 2 weeks shift towards earlier times during the year in better agreement with observations. These improvements in simulated LAI help to improve the simulated seasonal cycle of gross primary productivity (GPP) and as a result simulated net ecosystem productivity (NEP) as well.

1 Introduction

Biosphere-atmosphere interactions constitute a complex system which plays an important role in the regulation of the climate. These interactions are important determinants governing the physical and chemical properties of the atmosphere as well as the growth of plants, and result in the biosphere and atmosphere behaving as a coupled system (Pilegaard et al., 2003). Understanding this coupled behavior is a key research priority due, not only to the important role that terrestrial ecosystems play in modulating the global carbon cycle, but also to the significance of land surface characteristics for local and regional climate through biogeophysical effects (Cox et al., 2000; Prentice et al., 2001; Bonan, 2008; Franklin et al., 2016). This growing recognition of the role of land surface vegetation, and its bi-directional interactions with the climate system, has led to ever increasing complexity of the physical and biogeochemical processes that are incorporated in the land surface components of regional and global climate models (Foley et al., 1996; Sitch et al., 2008; Flato et al., 2013). Process-based land surface schemes and ecophysiological models (e.g., Running et al., 1999; Mäkelä et al., 2000; Friend et al., 2007; IPCC, 2013; Sato et al., 2015) simulate atmosphere-land exchanges of carbon, water, and energy, and offer tools for understanding vegetation behaviour for the present climate, and for projecting vegetation behaviour for future climate scenarios.

The plant canopy is a locus of physical and biogeochemical processes in an ecosystem. The functional and structural attributes of plant canopies are affected by microclimatic conditions, nutrient dynamics, herbivore activities, and many other factors (Asner et al., 2003). Leaves are the point of contact between plants and atmospheric CO_2; an increase in leaf area potentially enhances the opportunity for carbon uptake, albeit at the cost of a greater demand for water (Norby et al., 2003). The amount of foliage contained in plant canopies is one of the most basic ecological characteristics that integrates the effects of overall environmental conditions. Canopy leaf area serves as the dominant physical control over primary production (photosynthesis), transpiration, energy exchange, and other

41 physiological attributes pertinent to a range of ecosystem processes, and is therefore a core element of
42 ecological field and modeling studies (e.g., Knyazikhin et al., 1998; Xavier and Vettorazzi, 2004;
43 Aboelghar et al., 2010; Gonsamo and Chen, 2014; Bao et al., 2014; Savoy and Mackay, 2015).

44 LAI (defined as the amount of leaf area (m^2) in the canopy per unit ground area (m^2)) is a
45 dimensionless quantity and therefore can be assessed across a range of spatial scales, from individual
46 plant, a forest stand or grassland, to large regions and continents. Leaf phenology describes the
47 response of leaves to seasonal and climatic changes including the timing of bud burst, senescence (leaf
48 maturity or browning), and leaf abscission (leaf fall), and has been documented in a wide range of
49 literature (e.g., Kikuzawa, 1995; Myneni et al., 1997; Arora and Boer, 2005; Menzel et al., 2006;
50 Parmesan, 2006; Richardson et al., 2010; Dragoni et al., 2011; Smith and Hall, 2016). Leaf phenology
51 is a function of environmental conditions (in particular, temperature, soil moisture and day length). The
52 structural and adaptive qualities specific to vegetation type also determine the timing of leaf
53 phenological events. Accurate prediction of recurring vegetation cycles as a function of climate is an
54 important feature that vegetation models are expected to reproduce. The timing of bud burst and leaf
55 senescence determine the length of the growing season, and this affects gross and net primary
56 productivities (GPP and NPP), the annual cycle of LAI, and consequently, the energy, water, and
57 carbon fluxes. The seasonal progression of LAI also influences canopy conductance (Blanken and
58 Black, 2004), albedo (Sakai et al., 1997) and through its modulation of sensible and latent heat fluxes
59 (Moore et al., 1996) it also affects surface air temperatures (Levis and Bonan, 2004).

60 Despite its importance, the representation of LAI in terrestrial biosphere models is considered poor
61 (Richardson et al., 2012). Lack of high quality long term observations, the use of prescribed LAI,
62 simplified formulations of underlying biogeochemical processes, and coarse spatial resolution have
63 been mentioned as some of the limitations to accurate representation of LAI (Kucharik et al., 2006).
64 Since canopy seasonality is an important determinant of carbon (C) fluxes, poor representation of the

seasonal dynamics of LAI can lead to inaccurate estimation of vegetation productivity and consequently the net atmosphere-land CO_2 flux (Ryu et al., 2008).

Non-structural carbohydrates (NSCs) are the primary products of photosynthesis and a key energy source for plant growth and metabolism. NSCs play a central role in a plant's life processes and its response to the environmental conditions (Kozlowski, 1992; Ögren, 2000; Chatterton et al., 2006; O`Brien et al., 2014; Hartmann and Trumbore, 2016; Sperling et al., 2017). Previous studies have suggested that NSCs are stored in all plant organs (i.e., leaf, branch, root and stem) at different concentrations that vary seasonally and also inter-annualy in response to changes in environmental conditions (e.g., Oberhuber et al., 2011; Bazot et al., 2013; Mei et al., 2015). The amount of NSCs and their particular allocation to leaves, stems, and roots are considered eco-physiological traits and are among the range of adaptive strategies that plants use (Li et al., 2001; Poorter and Kitajima, 2007; Wyka et al., 2016). Many factors influence leaf NSC content, including nutrient elements (Zotz and Richter, 2006), temperature (Gough et al., 2010), precipitation (Würth et al., 2005), drought (Rosas et al., 2013), and phenology (Chen et al., 2017). NSC concentrations also vary seasonally and this seasonality has been observed in various plant species (e.g., Zhu et al., 2012; Richardson et al., 2013; Saffell et al., 2014). Despite this extensive research, the size and relative contributions of NSC pools across different tree organs and the movement of NSC amongst the tree organs are not well understood (Friedlingstein et al., 1999; Allen et al., 2005; Sala et al., 2012; Mei et al., 2015).

Plant NSC stores can compensate for a carbon or nitrogen shortage when current demand surpasses supply due to the seasonality of plant growth, stresses, or disturbances. The seasonal dynamics of NSC concentrations have been studied in various plant species (e.g., Zhu et al., 2012; Richardson et al., 2013; Saffell et al., 2014). In deciduous plants, when photosynthesis is constrained by limited leaf area and low temperature in early spring, NSC is mobilized from stem and roots to support respiration and tissue growth, resulting in decreased concentrations of NSC in these storage organs (Hoch et al., 2003;

89 Palacio et al., 2007). During the growing season, storage pools are replenished and NSC concentration
90 increases (Teixeira et al. 2007; Klein et al., 2016). Typically, NSC concentrations in storage organs of
91 the short-lived fast-growing species decrease in springtime after bud flush and then increase during the
92 remainder of the growing season. Correspondingly, the storage organs shift from being a NSC source
93 in the early growing season to becoming a sink in the late growing season, maintaining tree survival
94 after the termination of photosyntate flow from aboveground sources to supply energy for stem and
95 root tissues through the winter (Würth et al., 2005; Gough et al., 2010). During periods of limited
96 photosynthesis, such as winter dormancy or drought stress, trees depend solely on stored NSCs to
97 maintain basic metabolic functions, produce defensive compounds, and retain cell turgor (Sperling et
98 al., 2015). For deciduous species, the NSC storage provides the means to jump start leaf onset by using
99 a part of NSC stores to push leaves out at the onset of favourable weather conditions (e.g., in spring in
100 the northern hemisphere). Representation of NSC pools is therefore an essential step for terrestrial
101 biosphere models to better simulate leaf phenology and seasonal variability of LAI.

102 Models typically tend not to explicitly represent NSC pools (Le Roux et al., 2001) because of the
103 additional complexity that has to be dealt with unless it is necessary to do so for improved
104 physiological realism of the overall model or representation of a particular physiological process.
105 Those with explicit NSC pools (Dick and Dewar, 1992; Sampson et al., 2001; Ogle and Pacala, 2009;
106 Fisher et al., 2010) may choose to assign no metabolic cost associated with NSC pools and treat it
107 simply as a storage pool from which carbon can be used at a future time (Sala et al., 2012), or explicitly
108 account for the metabolic carbon costs associated with NSC pools. Existing representations of NSC
109 pools in models have aimed to maintain metabolic function through carbon deficit periods (Sampson et
110 al., 2001), achieve trade-offs between seedling growth and survivorship (Kobe, 1997; Fisher et al.,
111 2010), simulate stress tolerance to ozone (Retzlaff et al., 1996), and represent the response of the
112 respiration/photosynthesis ratio to increase in temperature (Dewar et al., 1999). Models have also used

mass balance of NSC pools as a trigger for plant mortality (Dick and Dewar, 1992; Cropper and Gholz, 1993; Sampson et al., 2001; Ogle and Pacala, 2009; Fisher et al., 2010). In terms of model structure, models may have only a single NSC storage pool (Cropper and Gholz, 1993; Kobe, 1997; Schaefer et al., 2008; Ogee et al., 2009) or multiple above- and below-ground pools (Le Dizès et al., 1997; Berninger et al., 2000; Allen et al., 2005). Biochemically, models vary in what the NSC pools correspond to. Most models do not distinguish between soluable (e.g., sugars) and insoluable (e.g., starch) NSCs, whereas others may make this distinction (Dick and Dewar, 1992; Le Dizès et al., 1997; Dewar et al., 1999; Levy et al., 2000; Génard et al., 2008; Schaefer et al., 2008). Dietze et al. (2014) provide a review of existing models which incorporate NSC pools within their framework.

Here, we include a representation of NSC pools and the associated parameterizations in the framework of the Canadian Land Surface Scheme-Canadian Terrestrial Ecosystem Model (CLASS-CTEM). CLASS-CTEM exhibits delayed leaf phenology and we attempt to address this issue. In the original model, the simulated global LAI reaches its maximum in August whereas the observed LAI peaks in July (e.g., see Fig. 11 of Anav et al., 2013). The objective of this study is to improve and assess the performance of CLASS-CTEM simulated leaf phenology for broadleaf cold deciduous trees. Model performance is evaluated against in situ measurements from three sites in~~from~~ the Fluxnet data network (*https://fluxnet.ornl.gov/obtain-data*) which provides tower-based meteorological variables used to drive the model as well as observations of LAI, carbon, and energy fluxes.

2 Model, data, and methods

2.1 CLASS-CTEM model

A coupled version of the Canadian Land Surface Scheme (v. 3.6; Verseghy, 2012) and Canadian Terrestrial Ecosystem Model (v. 2.1.1, Melton and Arora, 2014) (CLASS-CTEM) is used here. Slightly

137 older versions of both models are currently implemented in the second generation Canadian Earth
138 System Model (CanESM2; Arora et al., 2011). While CLASS simulates fluxes of energy, water, and
139 momentum at the land-atmosphere boundary, atmosphere-land fluxes of CO_2 and CH_4 are simulated by
140 CTEM. CLASS operates at a typical time step of 30 minutes and prognostically simulates the liquid
141 and frozen soil moisture and soil temperature for its multiple soil layers (3 layers are employed here
142 with maximum thicknesses of 0.1, 0.25 and 3.75 m); the temperature, thickness and fractional cover of
143 snow; and the temperature and amount of snow and rain on the vegetation canopy. The permeable
144 depth of the soil column may be smaller than the total depth of the soil layers employed; if a layer
145 spans the permeable depth boundary it is subdivided for hydrological calculations. CLASS
146 distinguishes four plant functional types (PFTs) (needleleaf trees, broadleaf trees, crops, and grasses) as
147 shown in Table 1. CLASS calculates net radiation (R_n) based on prognostically calculated land surface
148 albedo and the skin temperature of the land surface (T_s) as

149 $$R_n = SW(1-\alpha) + LW - \sigma T_s^4 \quad (1)$$

150 where α is albedo, SW and LW are incoming short and long wave radiation, σ is the Stefan-Boltzman
151 constant. R_n is partitioned into latent (LE), sensible (H), ground, and canopy heat fluxes. When in
152 equilibrium and over annual and longer time periods, since ground or canopy do not gain or lose heat
153 systematically, the sum of latent and sensible heat fluxes equals net radiation (R_n = LE + H).

154 CTEM simulates terrestrial ecosystem processes by prognostically tracking carbon in three living
155 vegetation components (leaves, stems and roots) and two dead carbon pools (litter and soil) for seven
156 non-crop and two crop PFTs that map directly onto CLASS' PFTs (Table 1). The terrestrial ecosystem
157 processes simulated in this study include photosynthesis, autotrophic respiration, heterotrophic
158 respiration, dynamic leaf phenology, and allocation of carbon from leaves to stem and root
159 components. These processes are described in a sequence of papers detailing parameterization of

160 photosynthesis, autotrophic and heterotrophic respiration (Arora, 2003), dynamic root distribution
161 (Arora and Boer, 2003), phenology, carbon allocation, biomass turnover and conversion of biomass to
162 structural attributes (Arora and Boer, 2005). A full description of CTEM can be found in the appendix
163 of Melton and Arora (2016) for CO_2 related processes and Arora et al. (2018) for CH_4 related
164 processes.

165 The structure of CTEM is shown in Fig. 1; the original three live vegetation pools (leaves, stem,
166 and roots) are indicated by L, S, and R subscripts, respectively), and the two dead carbon pools (litter
167 or detritus and soil carbon) are indicated by D and H subscripts, respectively). Time varying fluxes in
168 and out of these carbon pools (C_L, C_S, C_R, C_D, and C_H; in $kgCm^{-2}$) makes them prognostic variables in
169 the model. The corresponding rate change equations for amount of carbon in the three live vegetation
170 components (leaves, stem, and roots) in the original model version are represented by

171 $$\frac{dC_i}{dt} = a_{f_i}\left(G - E_m - E_g\right) - D_i = a_{f_i} N - D_i \quad (2)$$

172 where the index i corresponds to each of the live vegetation pools ($i = L, S, R$), a_{f_i} represents allocation
173 fraction for a given vegetation component, E_m is vegetation maintenance respiration, E_g is vegetation
174 growth respiration, D_i represents the litter loss. G is canopy gross primary productivity and the primary
175 photosynthetic carbon flux which drives all other carbon fluxes in and out of the model's various pools.
176 Although photosynthesis is a function of the total leaf area (LA, m^2), model parameterizations use LAI
177 (m^2/m^2) since all carbon fluxes and pools are represented per unit land area.

178 $N = G - E_m - E_g$ is the canopy net primary productivity (NPP) and therefore $a_{f_i} N$ represents fraction
179 of NPP allocated to the three vegetation components. Growth respiration, E_g, is estimated as a fraction
180 of the positive gross canopy photosynthetic rate after maintenance respiration has been accounted for
181 (equation A28, Melton and Arora (2016)). $E_a = E_m + E_g$ is the autotrophic respiration, therefore,

$N = G - E_a$. When heterotrophic respiration (E_h) is accounted for, net ecosystem productivity (NEP) is calculated as $NEP = G - E_a - E_h = N - E_h$. Positive NEP values indicate that land is gaining carbon from the atmosphere. Combined autotrophic and heterotrophic respiration ($E_a + E_h$) are referred to as the ecosystem respiration (E_r).

2.1.1 Addition of NSC pools

For the modifications made in this study, first, NSC pools are included in each of the live vegetation components (leaves, stem, and roots). The total biomass (Kg C m^{-2}) for each of these components is divided into its non-structural and structural components (indicated by subscripts NS and S) as shown in Figure 1. $C_L = C_{L,NS} + C_{L,S}$ and similarly for C_S and C_R. The fraction of NPP allocated to each live vegetation component is first moved to its non-structural part, and a flux of carbon from the non-structural to the structural part provides carbon to the structural part. Once the carbon is moved from non-structural to a structural part of a component it cannot be moved back. Since NPP includes respiratory losses, this essentially implies that respiratory carbon losses are assumed to occur from the non-structural part. This is consistent with observational and other modelling studies (e.g., Hoch et al., 2003; Sperling et al., 2015; Li et al., 2016) which show that plants' NSC stores become depleted due to respiration during dormant season and environmental stresses associated with cold temperatures and drought conditions. Litter losses in the model, on the other hand, occur from both the structural and non-structural parts of leaves, stem and root components.

The modified rate change equations for carbon in the non-structural and structural parts of leaf (Eq. 3) and stem and root (Eq. 4) components are thus written as

$$\begin{aligned}\frac{dC_{L,NS}}{dt} &= a_{f_L} N - D_{L,NS} - F_{ns2s,L} + T_S + T_R \\ \frac{dC_{L,S}}{dt} &= F_{ns2s,L} - D_{L,S}\end{aligned} \quad (3)$$

$$\begin{aligned}\frac{dC_{j,NS}}{dt} &= a_{f_i} N - D_{j,NS} - F_{ns2s,j} - T_j \\ \frac{dC_{j,S}}{dt} &= F_{ns2s,j} - D_{j,S}\end{aligned} \quad ; j = S, R \quad (4)$$

where $F_{ns2s,i}(i = L, S, R)$ represents carbon flux from the non-structural to structural part of a component (leaf, stem or root), and $T_j(j = S, R)$ represents the reallocation (or transfer) of carbon from stem and root components to leaves during leaf out period (see section 2.1.2). Note that there are no autotrophic respiration terms in equations (3) and (4) since they are already included in the term *N*, the net primary productivity. $F_{ns2s,i}$ is represented as

$$F_{ns2s,i} = \mu_i a_{f_i} N \max\left[0, (\eta - \eta_{i,min})\right] \quad (5)$$

where μ_i is a non-dimensional coefficient set to 70. Equation (5) attempts to keep the fraction of non-structural to total carbon in a component $\eta_i = C_{i,NS}/C_i$ above its minimum specified value $\eta_{i,min}$. During periods of negative NPP, for e.g. as is the case during winter for cold deciduous trees when they do not have their leaves on, $F_{ns2s,i}$ is set to zero. This represents the attempts by plants to conserve their NSC pools during a period of no productivity. The amount of carbon in non-structural and structural parts of all vegetation components are time varying variables and therefore so is the ratio of non-structural to total carbon (η_i). The minimum ratio of non-structural to total carbon in a component ($\eta_{i,min}$) is specified to be 0.05 for the broadleaf cold deciduous PFT considered here, following Li et al. (2016).

The above modifications made to version 2.1.1 of CTEM in regards to the inclusion of NSC pools allow the movement of non-structural carbohydrates between the model's three live vegetation components, in particular, reallocation of non-structural carbohydrates from stem and root components for leaf out at the onset of spring for the broadleaf cold deciduous tree PFT. Distinction between sugar and starch components of NSC pools is not made. This distinction is not necessary to achieve our primary objective of including NSC pools which is to address the issue of delayed phenology. In addition to incorporating NSC pools, we also adjust allocation fractions for the leaves, stem and root components after summer solstice in response to day length, and adjust the lower temperature threshold for leaf litter generation due to cold stress. Deciduousness at high latitudes is determined both by day length and temperature (Xie et al., 2015) and these modifications, discussed below, help to improve simulated leaf phenology.

2.1.2 Reallocation of non-structural carbon during leaf out period

Leaf phenology in CTEM is represented via four phenological states a plant can be in at any given time (Arora and Boer, 2005). These stages include no leaves or dormant state, maximum leaf growth state, normal growth state, and leaf fall or harvest state. Depending on their deciduousness, CTEM's nine plant functional types (Table 1) may or may not go through these four different leaf phenological states. A broadleaf cold deciduous tree, transitions through all four states in a year: leafless/dormant state in winter, maximum growth state (following arrival of favorable climatic condition in spring when all NPP is allocated to leaves), normal growth state (after reaching a threshold LAI, NPP is dynamically allocated to stem and roots in addition to leaves, and finally the leaf fall state (triggered by unfavorable environmental conditions and with no carbon allocation to leaves). When all the leaves have been shed, the trees go back into the leafless or dormant state again and the cycle repeats itself in

the next year. The phenology module of CLASS-CTEM model is explained in detail in Melton and Arora (2016).

In the original version of the model, when a plant moves into the maximum leaf growth state all NPP is allocated to leaves until a threshold LAI (L_{thrs}, m^2/m^2) has been grown. L_{thrs} is about 40%-50% of the maximum LAI a plant can support depending on its stem and root biomass and based on an allometric relationship between green and woody biomass (Melton and Arora, 2016). In the absence of NSC pools in the original model version, photosynthesis during the early leaf out period is based on a small imaginary amount of leaves (referred to as storage LAI). Once the actual LAI exceeds the storage LAI then photosynthesis is based on the actual LAI. Storage LAI is proportional to a plant's stem and root biomass and was intended as a proxy for the size of NSC pools. However, the rate of photosynthesis from a reasonably apportioned storage LAI is still too small to realistically 'push out' leaves at the onset of spring in a time period of about two weeks as seen in observations. This limitation in the original model version is overcome here with the inclusion of NSC pools. In the modified version of the model used here, a specified fraction of carbon amount needed to reach the threshold LAI is reallocated ($T_j, j=S, R$) from a plant's stem and root NSC pools to the non-structural part of leaves every day until LAI reaches L_{thrs}. Note that while this reallocation occurs the leaves are still able to photosynthesize and able to increase their biomass as in the original model version, depending on meteorological conditions. The objective of carbon reallocation from stem and roots to leaves is to accelerate the rate of leaf expansion and LAI increase during leaf onset.

The amount of carbon reallocated (kg C/m^2) from stem and root components to leaves is given by

$$T_j = \beta \frac{L_{thrs}}{SLA} f_j;\ j = S, R \tag{6}$$

$$f_j = \left\{ \begin{array}{cc} \frac{C_{j,NS}}{C_{S,NS} + C_{R,NS}} & if\ \eta_j > \eta_{j,min} \\ 0 & if\ \eta_j \leq \eta_{j,min} \end{array} \right\};\ j = S, R \tag{7}$$

where SLA is the specific leaf area (m^2/kg C), β is the reallocation coefficient set to 6.66×10^{-3} and fractions $f_j (j = S, R)$ ensure that carbon reallocated from stem and root NSC pools is proportional to the size of their NSC pools. Equation (7) also shows that when the fraction of NSC pool relative to total carbon in a component $(\eta_j = C_{j,NS}/C_j), j = S, R$ is equal to or drops below its minimum specific value $(\eta_{j,min})$ then reallocation is stopped. Reallocation is only performed during the leaf out state when trees are in the maximum leaf growth state.

2.1.3 Adjustments to allocation fraction to leaves after the summer solstice

CTEM uses dynamically calculated allocation fractions (Arora and Boer, 2005; Melton and Arora, 2016) for leaves, stem, and roots, which are based on the light, water, and leaf phenological status of vegetation. The allocation to the three live vegetation components is based on assumptions that carbon is preferentially allocated: 1) to roots when soil moisture is limiting, 2) to leaves when LAI is low, and 3) to stem to increase vegetation height and lateral spread when increasing LAI leads to a decrease in light penetration. These allocation fractions are superseded by three additional rules: 1) all carbon is allocated to leaves at the time of leaf out for cold deciduous tree PFTs to accelerate leaf development, 2) allocation fractions are adjusted when necessary to ensure a tree has enough stem and root biomass

to support leaves (to satisfy a structural allometric relationship), and 3) a minimum realistic root to shoot ratio is maintained for all PFTs.

The seasonality of globally-averaged LAI is dominated by the response of northern hemisphere's vegetation to increasing temperatures in spring and decreasing temperatures in autumn. When compared to observation-based estimates of globally-averaged LAI, the CLASS-CTEM simulated LAI starts to increase later in spring, shows a peak in August (as compared to July in observation-based estimates) and a much slower rate of decline after reaching its annual maximum, which typically occurs just after the summer solstice in each hemisphere (Fig. 11 of Anav et al., 2013). This last issue is addressed by reducing allocation fraction for leaves (a_{f_L}) of cold deciduous tree PFTs after summer solstice by multiplication with a day-length dependent factor (Γ) given by

$$\Gamma = \left[\frac{d}{d + (d_{max} - d)\,0.5\left(\tanh\left(\frac{\pi}{180}(20\phi - 800)\right) + 1\right)} \right]^{20} \tag{8}$$

$$d = 24 - \frac{24}{\pi} acos\left[max\left(-1, min\left(\frac{sin\phi \sin\delta_c}{cos\phi cos\,\delta_c}, 1\right)\right)\right] \tag{9}$$

where d is the day length at latitude ϕ (radian), d_{max} is its maximum value (hour), and δ_c (radians) is solar declination. Γ varies between 0 and 1 and its behaviour in Figure 2 shows how allocation to leaves is reduced at a faster (slower) rate closer to poles (equator) after summer solstice in the northern hemisphere (June 21). Below 30°N in the northern hemisphere equation (8) yields $\Gamma = 1$ so allocation fraction for leaves is not modified. Deciduousness due to day length and temperature typically does not occur in tropics where it is primarily controlled by soil moisture. Neither do broadleaf deciduous cold trees typically exist in the tropics. Similar behaviour is obtained for the southern hemisphere after December 21. Since the allocation fractions for leaves, stem, and root components should add to 1, a

decrease in allocation fraction for leaves implies an increase in allocation fraction for stem and root components in the modified version of the model. The use of summer solstice to initiate changes in plant behavior is reasonable since summer solstice is a trigger for many plant physiological processes. Adjustments to allocation fraction for leaves after summer solstice have also been made by Gim et al. (2017) (their equation (6)). Luo et al. (2018) showed that summer solstice marks a seasonal shift in plant growth, leaf physiology, and foliage turnover in temperate and boreal forests.

In the original version of the CLASS-CTEM model, continuous allocation of carbon to leaves up to the time until they are completely shed led to increase in LAI throughout the growing season rather than a near constant value or slowly decreasing LAI after the summer solstice.

2.1.4 Adjustments to the lower air temperature threshold

The CLASS-CTEM model is able to respond to environmental conditions and to transition between different leaf phenological states (Arora and Boer, 2005). Leaf litter (D_L) generation is caused by normal turnover of leaves as well as drought and cold stresses which all contribute to LAI seasonality.

$$D_L = C_L \left[1 - e^{\left(-\Omega_N - \Omega_C - \Omega_D\right)}\right] \quad (10)$$

where C_L is the leaf carbon pool and $\Omega_{N,C,D}$ are the leaf loss rates (day^{-1}) associated with normal (N) turnover of leaves and the cold (C) and drought (D) stresses. The leaf loss rate associated with cold stress (Ω_C) is based on Eqs. A49-50 of Melton and Arora (2016) (shown below as Eq. 11)

$$\Omega_C = \Omega_{C,max}\, L_{cold}^3 \quad (11)$$

where $\Omega_{C,max}$ is the maximum leaf loss rate due to cold stress and L_{cold} is a scalar that varies between 0 and 1 as follows

$$L_{cold} = \begin{cases} 1 & , T_a < \left(T_{cold}^{leaf} - 5\right) \\ 1 - \dfrac{T_a - \left(T_{cold}^{leaf} - 5\right)}{5} & , \left(T_{cold}^{leaf} - 5\right) < T_a < T_{cold}^{leaf} \\ 0 & , T_{cold}^{leaf} < T_a \end{cases} \quad (12)$$

T_{cold}^{leaf} is a PFT dependent parameter below which a PFT experiences damage to its leaves and this promotes leaf loss due to cold stress in the model.

The original version of the model used a T_{cold}^{leaf} parameter value of 8 °C throughout the year. In the modified version of the model used here for the broadleaf cold deciduous tree PFT a T_{cold}^{leaf} value of 12 °C is used after summer solstice. For broadleaf cold deciduous tree PFT, leaf out starts in spring, the maximum LAI occurs between July to September (during the northern hemisphere's summer) and the leaves are shed between October and November during autumn. Increasing T_{cold}^{leaf} leads to more leaf litter generation due to the cold stress in the autumn and moves the descending side of the LAI curve inwards during autumn.

2.2 Model evaluation and experimental set up

2.2.1 Description of Fluxnet sites

We evaluate the performance of the original and modified versions of the CLASS-CTEM framework in simulating leaf phenology at three well studied sites in the Eastern United States which are selected from the Fluxnet network: (1) Harvard Forest (US-Ha1) located at 42.53 ºN and 72.17 ºW, (2) Morgan Monroe State Forest (US-MMS) at 39.32 ºN and 86.41 ºW, and (3) University of Michigan Biological Station (US-UMB) at 45.55 ºN and 84.71 ºW. The location of the three Fluxnet sites is shown in Figure 3. The selected sites meet our requirement of availability of observation-based LAI data (against which our model results can be evaluated) and are primarily characterized by deciduous

broadleaf forests although with different species composition. The LAI measurements are based on an LAI-2000 plant canopy analyzer instrument and details are provided in Urbanski et al. (2007), Schmid et al. (2000), and Gough et al. (2008) for the Harvard Forest, Morgan Monroe, and University of Michigan sites, respectively. The mean annual climate at these sites and their species composition are summarized in Table 2. While these sites differ somewhat in the climate they experience, they share enough commonalities in climate to exhibit similar seasonal dynamics of LAI. Annual precipitation at these temperate locations (US-Ha1, US-MMS, and US-UMB) is 1189, 1083, and 613 mm, with an annual mean temperature of 8.2, 12.4, and 7.2 ºC for each site, respectively. These annual averages are based on the half-hourly meteorological data that are used to drive the CLASS-CTEM model for the time period summarized in Table 2.

The US-Ha1 site is owned by Harvard University. Most of its surrounding area was cleared for agriculture during European settlement in 1600-1700. The trees at the site have been regrowing since before 1900 and are currently characterized by predominantly red oak and red maple, with patches of mature hemlock stand and individual white pine. Climate measurements have been made at the Harvard Forest since 1964. The US-MMS site is owned by the Indiana Department of Natural Resources. Many of trees in the tower footprint are 60-80 years old. Today, the forest is a secondary successional broadleaf forest within the maple-beech to oak-hickory transition zone of the eastern deciduous forest. Finally, the US-UMB site is located within a protected forest owned by the University of Michigan and consists of mid-aged northern hardwoods, conifer understory, aspen, and old growth hemlock.

The permeable soil depths are specified at 2.5, 2.5, 2.62 m at the US-Ha1, US-MMS, and US-UMB sites, respectively. Soil texture information was adapted from the global data set of Zobler (1986) and used to specify the percentage of sand and clay in the model's three soil layers as follows. At US-Ha1,

370 the percentages of sand in the first, second and third soil layers are specified at 68.5, 66.5, and 72.25%,
371 and the percentage of clay at 5, 5 and 4.25%, respectively. At US-MMS, the percentages of sand in the
372 first, second and third soil layers are specified at 21, 22.5 and 30.25%, and the percentage of clay at 21,
373 23 and 23.75%, respectively. At US-UMB, the percentages of sand in the first, second and third soil
374 layers are specified at 71, 72.5 and 73.25%, and the percentage of clay at 7, 7 and 7.75%, respectively.
375
376 **2.2.2 CLASS-CTEM simulations**
377 For the three sites investigated here, we have used version 3.6 of the CLASS coupled to version
378 2.1.1 of the CTEM model and made changes mentioned above in Section 2.1. Model performance is
379 evaluated for both the modified and original (without NSC pools) versions against available
380 observation-based estimates of LAI, and energy and CO_2 fluxes. Simulations were performed for the
381 broadleaf cold deciduous tree PFT with 100% fractional cover.
382 Seven meteorological variables are required to drive the CLASS-CTEM model - air temperature,
383 air pressure, wind speed, incoming short wave radiation, incoming long wave radiation, precipitation,
384 and specific humidity. Fluxnet's gap-filled meteorological forcing was obtained for each of the three
385 ~~Fluxnet~~ sites. The data were either available at a half-hourly time step or were linearly interpolated
386 from hourly to half-hourly resolution. The meteorological data used to drive the model correspond to
387 the period 1998-2013 for the site in Harvard forest, 1999-2006 for the site in Morgan Monroe State
388 Forest and 1997-2013 for the site at the University of Michigan Biological Station.
389 All simulations were forced with meteorological data from their respective Fluxnet sites repeatedly
390 until model carbon pools reached equilibrium and the annually averaged NEP was close to zero. A
391 specified atmospheric CO_2 concentration of 350 ppm is used at all sites for this spin up. The real world
392 forests have, of course, experienced a gradual increase in atmospheric CO_2 concentration, changes in

climate, and disturbances over their life time. Although not perfect, in the absence of full histories of disturbance and meteorological data at these sites this approach still allows comparison of the seasonality of simulated LAI and primary carbon and energy fluxes with observation-based estimates once the model pools reach equilibrium. One caveat is that the modelled vegetation and soil carbon pools cannot be expected to be exactly the same as in the real world but we still expect them to be reasonable. We have chosen to use atmospheric CO_2 concentration of 350 ppm to spin up the model pools (while the average CO_2 concentration during the first decade of the 21st century was around 380 ppm) because the terrestrial biosphere is not in equilibrium with the atmospheric CO_2 concentration. The disturbance (fire) module was not activated in these simulations. Observation-based LAI measurements were obtained from the Ameriflux web site (*https://ameriflux.lbl.gov*). Energy and CO_2 fluxes were obtained from the Fluxnet web site (*https://fluxnet.fluxdata.org*).

3 Results

Model performance is evaluated by comparing simulated LAI and CO_2 fluxes of gross primary productivity (GPP) and net ecosystem productivity (NEP) which is our primary focus. We also compare radiative energy fluxes of net radiation and latent and sensible heat with their observation-based estimates from the modified and the original model versions.

3.1 LAI and land-atmosphere CO_2 fluxes

Figures 4-6 compare simulated values of LAI, GPP, NEP, and E_r from the two model versions with their observation-based estimates at the US-Ha1, US-MMS, and US-UMB Fluxnet sites. Observation-based measurements are shown in black and simulated mean daily values are shown in red (for the original model version indicated as CLASS-CTEM Original) and blue (for the modified version, with NSC pools and other changes indicated as CLASS-CTEM Modified). Just like simulated values, the

observation-based estimates also represent average daily values across all years for which the data were available. The mean annual values of LAI, GPP, E_r, and NEP are also summarized in Table 3. At all sites, when compared to the original version, the modified version of the model shows a phenological shift of about 2 weeks earlier in the year which is in better agreement with observed LAI transitions (Figs. 4-6, panel a). The timing of maximum LAI also improves and shows a shift of about 2 months earlier in the year, from late September and early October to late July and early August. The observation-based estimates of LAI suggest the presence of understory vegetation at two of the three Fluxnet sites (the Monroe and the Michigan sites). The CLASS-CTEM modelling framework does not represent any understory vegetation. Despite this, the model still overestimates maximum LAI at all locations and its implications are discussed further down. At all three sites, the inclusion of non-structural carbon pools (section 2.1.1) and other model modifications (sections 2.1.2 to 2.1.4) produces a notable improvement in simulated LAI seasonality, especially during canopy development (i.e., spring and early summer) and its autumn decline.

The Morgan Monroe site (Fig. 5) experiences somewhat warmer temperatures than the Harvard and Michigan sites (Figs. 4 and 6) (mean annual temperature at the Morgan Monroe is about 4 ºC higher than at the other two sites, see Table 2) and as a result the growing season is somewhat longer at the Morgan Monroe site. The model is able to successfully capture this difference amongst the sites. Overall, the simulated GPP and NEP (Figs. 4-6, panels b and c) compare reasonably well with observations. Improvements in simulated LAI seasonality lead to concomitant improvements in simulated GPP especially at the ascending side of the plots when the growing season starts. In the original version of the model the increase in GPP at the start of the growing season is delayed due to delayed leaf out. Note that the simulated GPP values compare well with their observation-based estimates despite the higher simulated LAI. Improvements in simulated GPP also lead to improvements

in simulated NEP in Figures 4-6 (panel c), and similar to GPP, especially on the ascending side of the plots at the start of the growing season.

The comparison with observation-based estimates of LAI and GPP is not completely straightforward since the observation-based estimates of these two quantities are put together by different communities and the fact that GPP is a derived quantity (as opposed to NEP which is directly observed). As a result, the observation-based estimates of LAI and GPP are not completely consistent with each other. This is seen in Figure 5 for the US-MMS site where the modified version of the model results in a better match with observation-based estimate of LAI (Fig. 5, panel a), but it shows a bias towards an early increase in GPP (Fig. 5, panel b). In contrast, in Figure 6, the simulated GPP in the modified version of the model compares better with its observation-based estimate than the LAI. In this respect, NEP provides a better measure to assess model improvement than GPP. In Figures 4 to 6 improvements in simulated LAI in the modified version of the model are more consistent with improvements in simulated NEP.

The individual contributions of the three modifications, 1) inclusion of NSC pools, 2) reduced allocation of carbon to leaves after summer solstice, and 3) change in parameter value of temperature threshold for leaf litter loss due to cold stress, made to the model for resulting improvements in LAI, GPP, and NEP are shown in the supplementary information.

The annual mean of observation-based NEP values (as shown in the figure legends of Figures 4 to 6) is positive because northern hemisphere temperate land is currently a sink of carbon (Myneni et al., 2001). In contrast, the annual mean of simulated NEP values is close to zero by construction, because the model was spun-up to an equilibrium state. The positive annual mean of observation-based NEP values, compared to simulated NEP values, can manifest in multiple ways – as primarily higher

summer values when NEP values are positive (as for the Harvard forest site), as higher values through the year (as is mostly the case at the Morgan Monroe site) and as less negative NEP values during non-growing season when NEP values are negative (as seen at the University of Michigan site). Regardless of this caveat, the inclusion of NSC pools to advance leaf onset and offset times does lead to an improvement in seasonality of simulated NEP values.

While photosynthesis primarily depends on the current meteorological conditions and LAI amongst other environmental factors (including atmospheric CO_2 concentration), ecosystem respiration (Figs. 4-6, panel d) depends strongly on the vegetation and soil carbon pool sizes. As a result, if simulated vegetation and soil carbon pools are larger or smaller than observation-based estimates then so would be the respiratory fluxes. Note also that the simulated annual respiratory fluxes are higher than observed at all three sites (Figs. 4-6, panel d, and Table 3). Had the simulated fluxes been lower than what they are now and closer to their observation-based estimates, then the simulated NEP would have been more similar to observations. Nevertheless, the model simulates the seasonality of ecosystem respiratory fluxes reasonably well. In absence of the long term disturbance history or meteorological data to drive the model with, the current methodology (where the model is driven repeatedly with the available observed meteorological data) is reasonable and allows us to assess the seasonality of simulated LAI and land-atmosphere CO_2 fluxes - which is the primary objective of our study.

3.2 NSC pools

Figures 7-9 evaluate the seasonal cycle of the NSC pools in leaf, stem, and root vegetation components at US-Ha1, US-MMS, and US-UMB Fluxnet sites, respectively. There are no observation-based estimates of NSC pools available at the three Fluxnet sites. For the broadleaf cold deciduous tree PFT considered here, the stem carbon pool is the largest (and so are its structural and non-structural parts) and the leaf carbon pool is the smallest (Figs. 7-9, panels a and c). The amount of non-structural

carbon reallocated from the stem and root NSC pools to leaves during leaf onset in early spring (see section 2.1.2) is shown in Figures 7-9 (panel b). Figures 7-9 (panel d) show the seasonality of the carbon flux from the non-structural to the structural part of the leaf, stem and root components for the three sites. The seasonality of total stem and root carbon pools is driven mostly by the seasonality of their non-structural parts.

For the stem and root components, the non-structural parts contribute about 6-10% to the total pool size. During the early leaf-out period when reallocation from stem and root NSC pools to leaves is taking place (section 2.1.2), the stem's NSC pool gets depleted. This transfer/reallocation stops after a threshold LAI is achieved. The transfer of NSC from stem and root pools to leaves occurs mostly through the stem (see Figs. 7-9, panel b) since its NSC pool is about 3-4 times larger than the root component. The NSC pool for both components reduces during the period when leaves are not present (and GPP is zero) due to respiratory and litter losses. The pools for both stem and root components get replenished later during the growing season when a sufficient amount of leaves has been grown and allocation of carbon to stem and root components is restored. This is seen in Figures 7-9 (panel d) which show the flux of carbon from non-structural to structural leaf, stem and root components. Early on during the growing season, carbon flux from the leaf NSC pool to its structural part is much higher since the model preferably allocates carbon to leaves as discussed in section 2.1.2. After a threshold LAI is reached, carbon is also allocated to stem and root NSC pools which subsequently start to allocate carbon to their structural pools and the tree biomass continues to increase. At the end of the growing season, when photosynthesis stops, allocation to all three components and the fluxes from NSC to structural parts terminate. During the dormant winter season NSC pools provide for the respiratory costs.

3.3 Energy fluxes

510 Figure 10 compares observation-based measurements of latent heat (LE), sensible heat (H), and net
511 radiation (R_n) fluxes at the three Fluxnet sites, with their simulated values from the two model versions.
512 Annual mean values of these observation-based and simulated radiative and turbulent energy fluxes are
513 also summarized in Table 3. Unlike the simulated fluxes, the annual mean sum of the observed LE and
514 H, averaged over the years for which observations are available, is not equal to the observed R_n. This
515 non-closure of the energy budget is seen at all three sites and is a typical characteristic of eddy
516 covariance based flux measurements (Gao et al., 2017). The annual energy budget closure is off by
517 17% at the University of Michigan Biological Station, by 20% at the Harvard Forest and by 30% at the
518 Morgan Monroe sites as seen in Table 3. Keeping this caveat in mind, the model overall captures the
519 seasonality of radiative and turbulent fluxes shown in Fig. 10 reasonably, with the exception of late
520 winter and early spring. During this period, as solar radiation increases R_n is underestimated (Fig. 10,
521 panels a-c) until the canopy approaches a full-leaf state and this leads to an underestimation of H (Fig.
522 10, panels g-i) and overestimation of LE. This may be caused by an overestimation of canopy
523 transmissivity and underestimation of snow and soil masking by leafless forests with increasing solar
524 elevation (recently observed in unpublished simulations with CLASS-CTEM at the Borden forest,
525 Borden, Ontario, Canada), and may also be exacerbated by the lack of representation of a small
526 evergreen needleleaf fraction at US-Hal and a conifer understory at US-UMB. LE is apparently
527 overestimated throughout the year at US-MMS but we suspect this reflects a larger underestimation of
528 LE relative to H in the measured fluxes; Oliphant et al. (2004) found that accounting for long sampling
529 tube damping effects on LE resulted in a 16% improvement in energy balance closure at this site. The
530 change to an earlier leaf phenology in the modified simulations results in a slightly earlier increase in
531 LE in the spring, as well as slightly earlier decreases in autumn at US-Hal and US-UMB, but
532 differences are much smaller at US-MMS.

In Figure 10 the changes in LAI, due to modifications made to the original version of the model, do not significantly affect latent heat fluxes because of two related reasons. First, at mid-high latitude locations where soil moisture constraint is not very large, as is the case at the three sites considered in this study, total evapotranspiration (or latent heat flux) is controlled by available energy. This is the reason for the expected seasonality in latent heat flux at these sites which is characterized by higher values during summer and lower values during winter. Second, since the latent heat flux at these three sites is controlled primarily by available energy, the resulting implication is that if evaporative demand cannot be met by transpiration then it will be met by evaporation from the soil. As a result, changes in LAI do not significantly affect total evapotranspiration but change the partitioning of evapotranspiration flux coming from transpiration, evaporation of intercepted water on canopy leaves, and evaporation from the soil.

4. Discussion and conclusions

The CLASS-CTEM model, similar to other land surface schemes implemented in other Earth system models, is not tuned for any specific location but is expected to behave realistically at all locations. Model processes correspond to generic PFTs, in this case broadleaf cold deciduous trees, and are not meant to represent specific species differences within a PFT. It is nearly impossible, at present, to determine model's~~the~~ more than 100 parameters for individual species. As a result, while our three chosen sites are characterized by different species (as shown in Table 2) they must be represented by a single set of parameter values which correspond to the broadleaf cold deciduous PFT.

Previous studies using the CLASS-CTEM model in the context of land-atmosphere CO_2 fluxes and simulated carbon pools have evaluated its performance at point (Arora, 2003; Arora and Boer, 2005;

555 Melton et al., 2015), regional (Garnaud et al., 2015; Peng et al., 2014; Arora et al., 2016) and global
556 (Arora and Boer, 2010; Melton and Arora, 2014, 2016) scales. These studies indicate that the model
557 performance is reasonable. CLASS-CTEM also participated in the TRENDY model intercomparison,
558 the result of which contributed to the Global Carbon project for years 2016 and 2017 (Le Quéré et al.,
559 2016, 2017). A typical model evaluation exercise at the global and regional scale compares model-
560 simulated geographical distribution of GPP, vegetation biomass, and soil carbon with their respective
561 observation-based estimates. Point scale studies, on the other hand, typically focus on the simulated
562 seasonality of energy and CO_2 fluxes as is the case in this study. Model evaluation exercises not only
563 help in identifying model limitations but also yield opportunities to improve model performance by
564 tuning model parameters.

565 We chose to perform equilibrium simulations by forcing the model repeatedly with available
566 meteorological data at specified CO_2 concentration of 350 ppm. In the absence of meteorological data
567 that shows a warming trend over the historical period we would not have been able to properly perform
568 a historical simulation. Our past experience shows that steady state simulations, as opposed to historical
569 transient simulations, allow an easier interpretation of model modifications in the absence of
570 confounding effects of changing climate and increasing CO_2.

571 Previous evaluations of the CLASS-CTEM model that highlighted its limitation of delayed leaf
572 phenology (e.g., Anav et al., 2013) were the motivation for this study. NSC pools play an important
573 role during leaf onset for broadleaf deciduous cold trees, but also other PFTs, and their effect in the
574 original model was represented using the concept of imaginary leaves whose LAI is assumed to be
575 directly proportional to non-leaf biomass. Here, we have included NSC pools in the model framework
576 explicitly along with some other changes and these modifications do lead to improvement in simulated
577 leaf phenology and concomitant improvements in simulated seasonal cycle of GPP and NEP.

578 Improvements in simulated energy fluxes are much harder to detect because the observation-based
579 energy fluxes are affected by non-closure of the energy budget but also because latent heat fluxes are
580 not as strongly dependent on LAI as GPP.

581 Despite the simulated LAI being higher than observation-based estimates the simulated GPP, E_r,
582 and NEP compare reasonably with their observation-based estimates. Possible reasons for higher
583 simulated LAI include higher than observed allocation to leaf compared to stem and root components
584 and lower than observed leaf turnover and/or leaf respiration rates. The model currently uses a
585 maximum carboxylation capacity ($V_{c,max}$, i.e., maximum photosynthetic rate) value of 57 u-mol CO_2/
586 m^2s for broadleaf cold deciduous trees based on Table 3 of Kattge et al. (2009) who derive $V_{c,max}$ values
587 for major PFTs using more than 700 data estimates. While in the CLASS-CTEM model photosynthesis
588 is also limited by light and transport capacity rates in addition to carboxylation capacity (see Appendix
589 A2 in Melton and Arora, 2016), $V_{c,max}$ remains a strong parameter and simulated GPP in the model is
590 proportional to $V_{c,max}$. While the model simulated LAI can be lowered by tuning allocation to leaves,
591 leaf turnover and/or respiration rates specifically for these sites, this would imply using a $V_{c,max}$ value
592 higher than that suggested by Kattge et al. (2009) to achieve realistic GPP. It is possible that the
593 average $V_{c,max}$ value derived by Kattge et al. (2009) is not representative of broadleaf cold deciduous
594 trees in the Eastern United States. The simulated LAI in the model is the result of multiple model
595 processes interacting with each other. We note this limitation of the model at these locations and plan
596 to address it in near future. While LAI is an important determinant of model performance even more
597 important are the land-atmosphere CO_2 fluxes from an ESM perspective since it is the CO_2 fluxes
598 which determine the carbon budget of the atmosphere in a fully coupled ESM simulation (Arora et al.,
599 2013).

Plants are extremely complex living organisms which respond to the changes in their physical and chemical environmental conditions using a myriad of adaptations. Our limited understanding of these adaptations comes only from empirical observations of their behaviour and measurement of their physical and chemical responses to environmental changes. Models typically represent only a fraction of this understanding because model structures depend on the purpose of the model and the amount of details that can be represented reasonably in a model's framework. In hindsight, the omission of NSC pools in the original model version was a structural error and while the conceptual imaginary leaves tried to mimic the fast growth rate of leaves during leaf onset at the arrival of favourable environmental conditions they were not completely successful in capturing the real-world behaviour. In addition, in a past exercise, we also used higher $V_{c,max}$ values at the beginning of the growing season to accelerate the rate of growth of leaves (based on Bauerle et al. (2012) and Alton (2017)) but this also did not help sufficiently to address the slower than observed rate of growth of LAI at the start of the growing season. Unlike physical models, which describe a physical process, modelling of biological response to changes in environmental conditions is more complex. While there may be underlying physical laws that determine the response of plants to changes in environmental conditions, we can only interpret this with a biological point of view. Dynamic vegetation models and land surface schemes parameterize biological functioning using mathematical formulations to reproduce empirical observations and modellers' conceptual understanding of how the biology works. The inclusion of NSC pools in the CLASS-CTEM framework is based on the same philosophy.

The implementation of NSC pools in the CLASS-CTEM modelling framework presented in this study is meant specifically to address the problem of delayed leaf phenology. NSC pools also play a vital role in the overall health of the plants as mentioned earlier in the introductory section. During periods of limited photosynthesis, trees depend solely on stored NSCs to maintain basic metabolic functions, produce defensive compounds, and retain cell turgor (Sperling et al., 2015). A period of

continuous drought, for instance, will gradually reduce the size of NSC pools and this can be used as a trigger to initiate drought related mortality in the model, or alternatively NSC pools may be used to allow leaf growth during a short-term dry period to represent resilience (Mitchell et al., 2013). The inclusion of NSC pools also lays the groundwork to implement a nitrogen (N) cycle in the CLASS-CTEM framework since modelling $V_{c,max}$ as a function of leaf N content requires leaf N content in the non-structural part of the leaves.

In conclusion, modifications to the CLASS-CTEM framework made in this study to address the problem of delayed leaf phenology yield improvements to simulated seasonality of LAI at the three Fluxnet sites considered here. These improvements, especially the inclusion of NSC pools also lay the groundwork for future model development and inclusion of new processes.

Acknowledgements

A. Asaadi was supported by a National Scientific and Engineering Research Council of Canada (NSERC) Visiting Postdoctoral Fellowship. We thank Fluxnet and AmeriFlux data networks for providing the data used in our study. We would also like to thank Philip Savoy for sharing LAI data for the Morgan Monroe site investigated in this study. We are also grateful to Reinel Sospedra-Alfonso and Michael Sigmond for providing comments on an earlier version of this manuscript.

641 **References**

642 Aboelghar, M., S. Arafat, A. Saleh, S. Naeem, M. Shirbeny, A. Belal, 2010: Retrieving leaf area index
643 from SPOT4 satellite data Egypt. *J. Remote Sens. Space Sci.,* **13,** 121–127.

644 Allen, M. T., P. Prusinkiewicz, T. M. DeJong, 2005: Using L-systems for modeling source-sink
645 interactions, architecture and physiology of growing trees: the L-PEACH model. *New Phytol.,*
646 **166,** 869–880.

647 Alton, P. B., 2017: Retrieval of seasonal rubisco-limited photosynthetic capacity at global FLUXNET
648 sites from hyperspectral satellite remote sensing: Impact on carbon modelling. *Agric. For.*
649 *Meteorol.,* **232,** 74–88.

650 Anav, A., and Coauthors, 2013: Evaluating the land and ocean components of the global carbon cycle
651 in the CMIP5 earth system models. *J. Climate*, **26**, 6801–6843.

652 Arora, V. K., 2003: Simulating energy and carbon fluxes over winter wheat using coupled land surface
653 and terrestrial ecosystem models, *Agr. Forest Meteorol.,* **118,** 21–47.

654 Arora, V. K., G. J. Boer, 2003: A representation of variable root distribution in dynamic vegetation
655 models, *Earth Interact.,* **7,** 1–19.

656 Arora, V. K., G. J. Boer, 2005: A parameterization of leaf phenology for the terrestrial ecosystem
657 component of climate models. *Global Change Biology,* **11,** 39–59.

658 Arora, V. K., G. J. Boer, 2010: Uncertainties in the 20th century carbon budget associated with land
659 use change, *Glob. Change Biol.,* **16,** 3327–3348.

660 Arora, V. K., J. F. Scinocca, G. J. Boer, J. R. Christian, K. L. Denman, G. M. Flato, V. V. Kharin, W.
661 G. Lee, W. J. Merryfield, 2011: Carbon emission limits required to satisfy future representative
662 concentration pathways of greenhouse gases, *Geophys. Res. Lett.,* **38,** L05805.

663 Arora, V. K., G. J. Boer, P. Friedlingstein, M. Eby, C. D. Jones, J. R. Christian, G. Bonan, L. Bopp, V.
664 Brovkin, P. Cadule, T. Hajima, T. Ilyina, K. Lindsay, J. F. Tjiputra, and T. Wu, 2013: Carbon-

concentration and carbon-climate feedbacks in CMIP5 earth system models. *J. Clim.* **26**, 5289–5314.

Arora, V. K., Y. Peng, W. A. Kurz, J. C. Fyfe, B. Hawkins, A. T. Werner, 2016: Potential near-future carbon uptake overcomes losses from a large insect outbreak in British Columbia, Canada. *Geophys. Res. Lett.,* **43,** 2590–2598.

Arora, V. K., J. R. Melton, and D. Plummer, 2018: An assessment of natural methane fluxes simulated by the CLASS-CTEM model, *Biogeosciences,* **15,** 4683-4709.

Asner, G. P., J. M. O. Scurlock, J. A. Hicke, 2003: Global synthesis of leaf area index observations: Implications for ecological and remote sensing studies. *Global Ecol. and Biogeo.,* **12,** 191–205.

Bao, Y., Y. Gao , S. Lü, Q. Wang, S. Zhang, J. Xu, R. Li, S. Li, D. Ma, X. Meng, H. Chen, Y. Chang, 2014: Evaluation of CMIP5 earth system models in reproducing leaf area index and vegetation cover over the Tibetan Plateau. *J. of Meteor. Research,* **28,** 1041–1060.

Bauerle, W. L., R. Oren, D. A. Way, S. S. Qian, P. C. Stoy, P. E. Thornton, J. D. Bowden, F. M. Hoffman, and R. F. Reynolds. 2012: Photoperiodic regulation of the seasonal pattern of photosynthetic capacity and the implications for carbon cycling. *Proc. Natl. Acad. Sci. U. S. A.,* 109(22):8612–8617.

Bazot, S., L. Barthes, D. Blanot, C. Fresneau, 2013: Distribution of non-structural nitrogen and carbohydrate compounds in mature oak trees in a temperate forest at four key phenological stages. Trees, 27, 1023–1034.

Berninger, F., E. Nikinmaa, R. Sievanen, P. Nygren, 2000: Modelling of reserve carbohydrate dynamics, regrowth and nodulation in a N_2-fixing tree managed by periodic prunings. *Plant Cell Environ.,* **23,** 1025–1040.

Blanken, P. D., T. A. Black, 2004: The canopy conductance of a boreal aspen forest, Prince Albert National Park, Canada. *Hydrol. Process.,* **18,** 1561–1578.

689 Bonan, G. B., 2008: Forests and climate change: forcings, feedbacks, and the climate benefits of
690 forests. *Science*, **320,** 1444-1449.
691 Chatterton, N. J., K. A. Watts, K. B. Jensen, P. A. Harrison, W. H. Horton, 2006: Nonstructural
692 carbohydrates in oat forage. *J. Nutr.,* **136,** 2111S–2113S.
693 Chen, Z., L. Wang, Y. Dai, X. Wan, S. Liu, 2017: Phenology-dependent variation in the non-structural
694 carbohydrates of broadleaf evergreen species plays an important role in determining tolerance
695 to defoliation (or herbivory). Scientific Reports, 7 (10125). doi:10.1038/s41598-017-09757-2.
696 Cox, P. M., R. A. Betts, C. D. Jones, S. A. Spall, I. J. Totterdell, 2000: Acceleration of global warming
697 due to carbon-cycle feedbacks in a coupled climate model. *Nature*, **408**, 184–187.
698 Cropper, W. P., H. L. Gholz, 1993: Simulation of the carbon dynamics of a Florida slash pine
699 plantation. *Ecol. Model.,* **66,** 231–249.
700 Dewar, R. C., B. E. Medlyn, R. E. McMurtrie, 1999: Acclimation of the respiration photosynthesis
701 ratio to temperature: insights from a model. *Glob. Change Biol.,* **5,** 615–622.
702 Dick, J. M., R. C. Dewar, 1992: A mechanistic model of carbohydrate dynamics during adventitious
703 root development in leafy cuttings. *Ann. Bot.,* **70,** 371–377.
704 Dietze, M. C., A. Sala, M. S. Carbone, C. I. Czimczik, J. A. Mantooth, A. D. Richardson, and R.
705 Vargas, 2014: Nonstructural carbon in woody plants. *Annual review of plant biology,* **65,** 667-
706 687.
707 Dragoni, D., H. P. Schmid, C. A. Wayson, H. Potter, C. S. B. Grimmond, J. C. Randolph, 2011:
708 Evidence of increased net ecosystem productivity associated with a longer vegetated season in a
709 deciduous forest in south-central Indiana, USA. *Global Change Biol.,* **17,** 886–897.

710 Fisher, R., N. McDowell, D. Purves, P. Moorcroft, S. Sitch, P. Cox, C. Huntingford, P. Meir, F. I.
711 Woodward, 2010: Assessing uncertainties in a second-generation dynamic vegetation model
712 caused by ecological scale limitations. *New Phytol.,* **187,** 666–681.

713 Flato, G., J. Marotzke, B. Abiodun, P. Braconnot, S. C. Chou, W. Collins, P. Cox, F. Driouech, S.
714 Emori, V. Eyring, C. Forest, P. Gleckler, E. Guilyardi, C. Jakob, V. Kattsov, C. Reason, M.
715 Rummukainen; Evaluation of Climate Models, in Climate Change 2013: The Physical Science
716 Basis. Contribution of Working Group I to the Fifth Assessment Report of the
717 Intergovernmental Panel on Climate Change, edited by: T. F. Stocker, D. Qin, G.-K. Plattner,
718 M. Tignor, S. K. Allen, J. Boschung, A. Nauels, Y. Xia, V. Bex, P. M. Midgley. Cambridge
719 Univ. Press, Cambridge, United Kingdom and New York, NY, USA, 2013, pp. 741–866.

720 Foley, J. A., I. C. Prentice, N. Ramankutty, S. Levis, D. Pollard, S. Sitch, and A. Haxeltine, 1996: An
721 integrated biosphere model of land surface processes, terrestrial carbon balance and vegetation
722 dynamics. *Global Biogeochem. Cycles*, **10,** 603–628.

723 Franklin, J., J. M. Serra-Diaz, A. D. Syphard, H. M. Regan, 2016: Global change and terrestrial plant
724 community dynamics. *Proc. Natl. Acad. Sci.*, **113,** 3725–3734.

725 Friedlingstein, P., G. Joel, C. B. Field, I. Y. Fung, 1999: Toward an allocation scheme for global
726 terrestrial carbon models. *Glob. Change Biol.,* **5,** 755–770.

727 Friend, A., A. Arneth , N. Kiang , M. Lomas, J. Ogee, C. Roedenbeck, S. Running, J. Santaren, S.
728 Sitch, N. Viovy, I. Woodward, S. Zaehle, 2007: Fluxnet and modelling the global carbon cycle.
729 *Global Change Biol.,* **13,** 610–633.

730 Gao, Z., H. Liu, G. G. Katul, T. Foken, 2017: Non-closure of the surface energy balance explained by
731 phase difference between vertical velocity and scalars of large atmospheric eddies. *Environ.*
732 *Res. Lett.,* **12,** p. 034025.

733 Garnaud, C., L. Sushama, and D. L. Verseghy, 2015: Impact of interactive vegetation phenology on the
734 Canadian RCM simulated climate over North America. *Climate Dyn.*, **45**, 1471–1492.
735 Génard, M., J. Dauzat, N. Franck, F. Lescourret, N. Moitrier, P. Vaast, G. Vercambre, 2008: Carbon
736 allocation in fruit trees: from theory to modelling. *Trees,* **22,** 269–282.
737 Gim, H.-J., S. K. Park, M. Kang, B. M. Thakuri, J. Kim, and C.-H. Ho, 2017: An improved
738 parameterization of the allocation of assimilated carbon to plant parts in vegetation dynamics
739 for Noah-MP. *Journal of Advances in Modeling Earth Systems*, **9(4),** 1776–1794.
740 Gonsamo, A., J. M. Chen, 2014: Continuous observation of leaf area index at Fluxnet-Canada sites.
741 *Agric. For. Meteorol.,* **189,** 168–174.
742 Gough, C. M., C. S.Vogel, H. P. Schmid, H. B. Su, P. S. Curtis, 2008: Multi-year convergence of
743 biometric and meteorological estimates of forest carbon storage. *Agricultural and Forest*
744 *Meteorology,* **148,** 158–170.
745 Gough, C. M., C. E. Flower, C. S. Vogel, P. S. Curtis, 2010: Phenological and temperature controls on
746 the temporal non-structural carbohydrate dynamics of Populus grandidentata and Quercus
747 rubra. *Forests,* **1,** 65–81.
748 Hartmann, H., S. Trumbore, 2016: Understanding the roles of nonstructural carbohydrates in forest
749 trees - from what we can measure to what we want to know. *New Phytol.,* **211,** 386–403.
750 Hoch, G., M. Popp, C. Körner, 2002: Altitudinal increase of mobile carbon pools in *Pinus cembra*
751 suggest sink limitation at the Swiss treeline. *Oikos,* **98,** 361–374.
752 Hoch, G., A. Richter, C. Körner, 2003: Non-structural carbon compounds in temperate forest trees.
753 *Plant Cell Environ.,* **26,** 1067–1081.

754 IPCC, 2013: Summary for Policymakers. In: Climate Change 2013: The Physical Science Basis.
755 Contribution of Working Group I to the Fifth Assessment Report of the Intergovernmental
756 Panel on Climate Change [Stocker, T.F., D. Qin, G.-K. Plattner, M. Tignor, S. K. Allen, J.
757 Boschung, A. Nauels, Y. Xia, V. Bex and P.M. Midgley (eds.)]. Cambridge University Press,
758 Cambridge, United Kingdom and New York, NY, USA.
759 Kattge, J., W. Knorr, T. Raddatz, and C. Wirth, 2009: Quantifying photosynthetic capacity and its
760 relationship to leaf nitrogen content for global-scale terrestrial biosphere models. *Global*
761 *Change Biology,* **15,** 976–991.
762 Kikuzawa, K., 1995: Leaf phenology as an optimal strategy for carbon gain in plants. *Can. J. Bot.,* **73,**
763 158–163.
764 Klein, T., Y. Vitasse, G. Hoch, 2016: Coordination between growth, phenology and carbon storage in
765 three coexisting deciduous tree species in a temperate forest. *Tree Physiology,* **36,** 847–855.
766 Knyazikhin, Y., J. V. Martonchik, D. J. Diner, R. B. Myneni, M. Verstraete, B. Pinty, and N. Gobron,
767 1998: Estimation of vegetation canopy leaf area index and fraction of absorbed
768 photosynthetically active radiation from atmosphere-corrected MISR data, *J. Geophys. Res.,*
769 **103,** 32239–32256.
770 Kobe, R. K., 1997: Carbohydrate allocation to storage as a basis of interspecific variation in sapling
771 survivorship and growth. *Oikos,* **80,** 226–33.
772 Kozlowski, T. T., 1992: Carbohydrate sources and sinks in woody plants. *Bot. Rev.,* **58,** 107–222.
773 Kucharik C. J., C. C. Barford, M. E. Maayar, S. C. Wofsy, R. K. Monson, D. D. Baldocchi, 2006: A
774 multiyear evaluation of a dynamic global vegetation model at three ameriflux forest sites:
775 vegetation structure, phenology, soil temperature, and CO_2 and H_2O vapor exchange.
776 *Ecological Modelling* **196**, 1–31.

Le Dizès, S., P. Cruiziat, A. Lacointe, H. Sinoquet, X. Le Roux, et al., 1997: A model for simulating structure-function relationships in walnut tree growth processes. *Silva Fenn.,* **31,** 313–328.

Le Quéré, C., and Coauthors, 2016: Global Carbon Budget 2016, *Earth Syst. Sci. Data,* **8,** 605-649.

Le Quéré, C., and Coauthors, 2017: Global Carbon Budget 2017, *Earth Syst. Sci. Data Discuss.,* in review.

Le Roux, X., A. Lacointe, A. Escobar-Gutiérrez, S. Le Dizès, 2001: Carbon-based models of individual tree growth: a critical appraisal. *Ann. For. Sci.,* **58,** 469–506.

Levis, S., G. B. Bonan, 2004: Simulating springtime temperature patterns in the community atmosphere model coupled to the community land model using prognostic leaf area. *J. Clim.,* **17,** 4531–4540.

Levy, P. E., M. E. Lucas, H. M. McKay, A. J. Escobar-Gutierrez, A. Rey, 2000: Testing a process-based model of tree seedling growth by manipulating [CO_2] and nutrient uptake. *Tree Physiol.,* **20,** 993–1005.

Li, M. H., G. Hoch, C. Körner, 2001: Spatial variability of mobile carbohydrates within Pinus cembra trees at the alpine treeline. *Phyton,* **41,** 203–213.

Li, N., N. He, G. Yu, Q. Wang, J. Sun, 2016: Leaf non-structural carbohydrates regulated by plant functional groups and climate: evidences from a tropical to cold-temperate forest transect. *Ecological Indicators,* **62,** 22–31.

Luo, T., X. Liu, L. Zhang, X. Li, Y. Pan, and I. J. Wright, 2018: Summer solstice marks a seasonal shift in temperature sensitivity of stem growth and nitrogen-use efficiency in cold-limited forests. *Agricultural and Forest Meteorology,* 248, 469–478.

798 Mäkelä, A., J. Landsberg, A. R. Ek, T. E. Burk, M. Ter-Mikaelian, G. I. Ågren, C. D. Oliver, P.
799 Puttonen, 2000: Process-based models for forest ecosystem management: current state of the art
800 and challenges for practical implementation. *Tree Physiology,* **20,** 289–298.
801 Mei, L., Y. Xiong, J. Gu, Z. Wang, D. Guo, 2015: Whole-tree dynamics of non-structural carbohydrate
802 and nitrogen pools across different seasons and in response to girdling in two temperate trees.
803 *Oecologia,* **177,** 333–344.
804 Melton, J. R., V. K. Arora, 2014: Sub-grid scale representation of vegetation in global land surface
805 schemes: implications for estimation of the terrestrial carbon sink. *Biogeosciences,* **11,** 1021–
806 1036.
807 Melton, J. R., R. K. Shrestha, and V. K. Arora, 2015: The influence of soils on heterotrophic
808 respiration exerts a strong control on net ecosystem productivity in seasonally dry Amazonian
809 forests. *Biogeosciences,* **12,** 1151–1168.
810 Melton, J. R., V. K. Arora, 2016: Competition between plant functional types in the Canadian
811 Terrestrial Ecosystem Model (CTEM) v. 2.0, *Geosci. Model Dev.,* **9,** 323–361.
812 Menzel, A., and Coauthors, 2006: European phenological response to climate change matches the
813 warming pattern. *Global Change Biol,* **12,** 1969–1976.
814 Mitchell P. J., A. P. O'Grady, D. T. Tissue, D. A. White, M. L. Ottenschlaeger, E. A. Pinkard, 2013:
815 Drought response strategies define the relative contributions of hydraulic dysfunction and
816 carbohydrate depletion during tree mortality. *New Phytologist,* **197,** 862–872.
817 Moore, K. E., and Coauthors, 1996: Seasonal variation in radiative and turbulent exchange at a
818 deciduous forest in central Massachusetts. *J. Appl. Meteorol.,* **35,** 122–134.
819 Myneni, R. B., C. D. Keeling, C. J. Tucker, G. Asrar, R. R. Nemani, 1997: Increased plant growth in
820 the northern high latitudes from 1981 to 1991. *Nature,* **386,** 698–702.

821 Myneni, R. B., J. Dong, C. J. Tucker, R. K. Kaufmann, P. E. Kauppi, J. Liski, L. Zhou, V. Alexeyev,
822 and M. K. Hughes, 2001: A large carbon sink in the woody biomass of Northern forests. *Proc.*
823 *Natl. Acad. Sci.,* **98,** 14784-14789.
824 Norby, R. J., J. D. Sholtis, C. A. Gunderson, S. S. Jawdy, 2003: Leaf dynamics of a deciduous forest
825 canopy: no response to elevated CO2. *Oecologia,* **136,** 574–584.
826 Oberhuber, W., I. Swidrak, D. Pirkebner, A. Gruber, 2011: Temporal dynamics of nonstructural
827 carbohydrates and xylem growth in Pinus sylvestris exposed to drought. *Canadien Journal of*
828 *Forest Research,* **41,** 1590–1597.
829 O'Brien, M. J., S. Leuzinger, C. D. Philipson, J. Tay, A. Hector, 2014: Drought survival of tropical tree
830 seedlings enhanced by non-structural carbohydrate levels. *Nature Climate Change,* **4,** 710–714.
831 Ogee, J., M. M. Barbour, L. Wingate, D. Bert, A. Bosc, M. Stievenard, C. Lambrot, M. Pierre, T.
832 Bariac, D. Loustau, and R. C. Dewar, 2009: A single-substrate model to interpret intra-annual
833 stable isotope signals in tree-ring cellulose. *Plant Cell Environ.,* **32,** 1071–1090.
834 Ogle, K., S. W. Pacala, 2009: A modeling framework for inferring tree growth and allocation from
835 physiological, morphological and allometric traits. *Tree Physiol.,* **29,** 587–605.
836 Ögren, E., 2000: Maintenance respiration correlates with sugar but not nitrogen concentration in
837 dormant plants. *Physiol. Plant.,* **108,** 295–299.
838 Oliphant, A. J., C. S. B. Grimmond, H. N. Zutter, H. P. Schmid, H.-B. Su, S. L. Scott, B. Offerle, J. C.
839 Randolph, J. Ehman. 2004: Heat storage and energy balance fluxes for a temperate deciduous
840 forest. *Agric. For. Meteorol.,* **126,** 185-201.
841 Palacio, S., P. Millard, M. Maestro, G. Montserrat-Marti, 2007: Non-structural carbohydrates and
842 nitrogen dynamics in Mediterranean sub-shrubs: an analysis of the functional role of over
843 wintering leaves. *Plant Biol.,* **9,** 49–58.

844 Parmesan, C., 2006: Ecological and evolutionary responses to recent climate change. *Annual Review of*
845 *Ecology,* Evolution and Systematics, **37,** 637–669.
846 Peng, Y., V. K. Arora, W. A. Kurz, R. A. Hember, B. J. Hawkins, J. C. Fyfe, and A. T. Werner, 2014:
847 Climate and atmospheric drivers of historical terrestrial carbon uptake in the province of British
848 Columbia, Canada, *Biogeosciences,* **11,** 635-649.
849 Pilegaard, K., T. N. Mikkelsen, C. Beier, N. O. Jensen, P. Ambus, H. Ro-Poulsen, 2003: Field
850 measurements of atmosphere-biosphere interactions in a Danish beech forest. *Boreal*
851 *Environment Research,* **8,** 315–333.
852 Poorter, L., K. Kitajima, 2007: Carbohydrate storage and light requirements of tropical moist and dry
853 forest tree species. *Ecology,* **88,** 1000–1011.
854 Prentice, I.C., G.D. Farquhar, M.J.R. Fasham, M.L. Goulden, M. Heimann, V.J. Jaramillo, H.S.
855 Kheshgi, C. Le Quéré, R.J. Scholes, D.W.R. Wallace, D. Archer, M.R. Ashmore, O. Aumont,
856 D. Baker, M. Battle, M. Bender, L.P. Bopp, P. Bousquet, K. Caldeira, P. Ciais, P.M. Cox, W.
857 Cramer, F. Dentener, I.G. Enting, C.B. Field, P. Friedlingstein, E.A. Holland, R.A. Houghton,
858 J.I. House, A. Ishida, A.K. Jain, I.A. Janssens, F. Joos, T. Kaminski, C.D. Keeling, R.F.
859 Keeling, D.W. Kicklighter, K.E. Kohfeld, W. Knorr, R. Law, T. Lenton, K. Lindsay, E. Maier-
860 Reimer, A.C. Manning, R.J. Matear, A.D. McGuire, J.M. Melillo, R. Meyer, M. Mund, J.C.
861 Orr, S. Piper, K. Plattner, P.J. Rayner, S. Sitch, R. Slater, S. Taguchi, P.P. Tans, H.Q. Tian,
862 M.F. Weirig, T. Whorf, A. Yool, L. Pitelka, A. Ramirez Rojas, 2001: The Carbon Cycle and
863 Atmopsheric Carbon Dioxide. In: Climate Change 2001: The Scientific Basis. Contribution of
864 Working Group I to the Third Assessment Report of the Intergovernmental Panel on Climate
865 Change [Houghton, J.T., Y. Ding, D.J. Griggs, M. Noguer, P.J. van der Linden, X. Dai, K.
866 Maskell, and C.A. Johnson (eds.)]. Cambridge University Press, Cambridge, United Kingdom
867 and New York, NY, USA, 881pp.

868 Retzlaff, W. A., D. A. Weinstein, J. A. Laurence, B. Gollands, 1996: Simulated root dynamics of a
869 160-year-old sugar maple (Acer saccharum Marsh.) tree with and without ozone exposure using
870 the TREGRO model. *Tree Physiol.,* **16,** 915–921.
871 Richardson, A. D., and Coauthors, 2010: Influence of spring and autumn phenological transitions on
872 forest ecosystem productivity. *Philos. Trans. R. Soc. B,* **365,** 3227–3246.
873 Richardson, A. D., and Coauthors, 2012: Terrestrial biosphere models need better representation of
874 vegetation phenology: results from the North American Carbon Program Site Synthesis. *Global*
875 *Change Biol.,* **18,** 566–584.
876 Richardson, A. D., M. S. Carbone, T. F. Keenan, C. I. Czimczik, D. Y. Hollinger, P. Murakami, P. G.
877 Schaberg, X. Xu, 2013: Seasonal dynamics and age of stemwood nonstructural carbohydrates in
878 temperate forest trees. *New Phytologist,* **197,** 850–861.
879 Rosas, T., L. Galiano, R. Ogaya, J. Peñuelas, J. Martínez-Vilalta, 2013: Dynamics of non-structural
880 carbohydrates in three Mediterranean woody species following long-term experimental drought.
881 *Frontiers in Plant Science,* **4,** 1–16.
882 Running, S., D. Baldocchi, D. Turner, S. Gower, P. Bakwin, K. Hibbard, 1999: A global terrestrial
883 monitoring network integrating tower fluxes, flask sampling, ecosystem modelling and EOS
884 satellite data. *Remote Sens. Environ.,* **70,** 108–127.
885 Ryu, S. R., J. Chen, A. Noormets, M. K. Bresee, S. V. Ollinger, 2008: Comparisons between PnET-
886 Day and eddy covariance based gross ecosystem production in two Northern Wisconsin forests.
887 *Agric. For. Meteorol.,* **148,** 247–256.
888 Saffell, B. J., F. C. Meinzer, D. R. Woodruff, D. C. Shaw, S. L. Voelker, B. Lachenbruch, K. Falk,
889 2014: Seasonal carbohydrate dynamics and growth in Douglas-fir trees experiencing chronic,
890 fungal-mediated reduction in functional leaf area. *Tree Physiol.,* **34,** 218–228.

Sakai, R. K., D. R. Fitzjarrald, K. E. Moore, 1997: Detecting leaf area and surface resistance during transition seasons. *Agric. For. Meteorol.,* **84,** 273–284.

Sala, A., D. R. Woodruff, F. C. Meinzer, 2012: Carbon dynamics in trees: feast or famine? *Tree Physiol.,* **32,** 764–775.

Sampson, D. A., K. H. Johnsen, K. H. Ludovici, T. J. Albaugh, C. A. Maier, 2001: Stand-scale correspondence in empirical and simulated labile carbohydrates in loblolly pine. *For. Sci.,* **47,** 60–68.

Sato, H., A. Ito, A. Ito, T. Ise, E. Kato, 2015: Current status and future of land surface models. *Soil Sci. Plant Nutr.*, **61,** 34–47.

Savoy, P., D. S. Mackay, 2015: Modeling the seasonal dynamics of leaf area index based on environmental constraints to canopy development. *Agric. For. Meteorol.,* **200,** 46–56.

Schaefer, K., G. J. Collatz, P. Tans, A. S. Denning, I. Baker, J. Berry, L. Prihodko, N. Suits, and A. Philpott, 2008: Combined simple biosphere/Carnegie-Ames-Stanford approach terrestrial carbon cycle model. *J. Geophys. Res.,* **113,** G03034.

Schmid, H. P., C. S. B. Grimmond, F. Cropley, B. Offerle, H. B. Su, 2000: Measurements of CO_2 and energy fluxes over a mixed hardwood forest in the mid-western United States. *Agricultural and Forest Meteorology,* **103,** 357–374.

Sitch, S., C. Huntingford, N. Gedney, P. E. Levy, M. Lomas, S. L. Piao, R. Betts, P. Ciais, P. Cox, P. Friedlingstein. C. D. Jones, I. C. Prentice, F. I. Woodward, 2008: Evaluation of the terrestrial carbon cycle, future plant geography and climate-carbon cycle feedbacks using five Dynamic Global Vegetation Models (DGVMs). *Glob. Change Biol.,* **14,** 2015-2039.

Smith, L. M., S. Hall, 2016: Extended leaf phenology may drive plant invasion through direct and apparent competition. *Oikos,* **125,** 839–848.

914 Sperling, O., J. M. Earles, F. Secchi, J. Godfrey, M. A. Zwieniecki, 2015: Frost induces respiration and
915 accelerates carbon depletion in trees. *PLoS One,* 10:e0144124.
916 Sperling, O., L. C. R. Silva, A. Tixier, G. Théroux-Rancourt, M. A. Zwieniecki, 2017: Temperature
917 gradients assist carbohydrate allocation within trees. *Sci. Rep.,* **7** (3265). doi:10.1038/s41598-
918 017-03608-w
919 Teixeira, E. I., D. J. Mott, M. V. Mickelbart, 2007: Seasonal patterns of root C and N reserves of
920 lucerne crops (Medicago sativa L.) grown in a temperate climate were affected by defoliation
921 regime. *Eur J Agron,* **26,** 10–20.
922 Urbanski, S., and Co-authors, 2007: Factors controlling CO_2 exchange on timescales from hourly to
923 decadal at Harvard Forest. *Journal of Geophysical Research-Biogeosciences,* **112,** G02020.
924 Verseghy, D., 2012: CLASS – the Canadian Land Surface Scheme (Version 3.6), Technical
925 Documentation, Tech. rep., Science and Technology Branch, Environment Canada.
926 Würth, M. K. R., S. Peláez-Riedl, S. J. Wright, C. Körner, 2005: Non-structural carbohydrate pools in a
927 tropical forest. *Oecologia,* **143,** 11–24.
928 Wyka, T. P., P. Karolewski, R. Żytkowiak, P. Chmielarz, J. Oleksyn, 2016: Whole-plant allocation to
929 storage and defense in juveniles of related evergreen and deciduous shrub species. *Tree*
930 *Physiology,* **36,** 536–547.
931 Xavier, A. C., and C. A. Vettorazzi, 2004: Mapping leaf area index through spectral vegetation indices
932 in a subtropical watershed. International J. of Remote Sensing, 25, 1661–1672.
933 Xie, Y., X. Wang, and J. A. Silander, 2015: Deciduous forest responses to temperature, precipitation,
934 and drought imply complex climate change impacts. *Proc. Natl. Acad. Sci.,* **112,** 13585–13590.
935 Zhu, W. Z., M. Cao, S. G. Wang, W. F. Xiao, M. H. Li, 2012: Seasonal dynamics of mobile carbon
936 supply in Quercus aquifolioides at the upper elevational limit. *PLoS ONE,* **7,** e34213.

937 Zobler, L., 1986: A world soil file for global climate modelling. NASA Technical Memorandum
938 87802. NASA Goddard Institute for Space Studies, New York, New York, U.S.A.
939 Zotz, G., A. Richter, 2006: Changes in carbohydrate and nutrient contents throughout a reproductive
940 cycle indicate that phosphorus is a limiting nutrient in the epiphytic bromeliad. *Werauhia*
941 *sanguinolenta. Ann. Bot.,* **97,** 745–754.

List of Tables

Table 1: Plant functional types (PFTs) represented in CTEM and their relation to CLASS PFTs.

CLASS PFTs	CTEM PFTs
Needleleaf trees	Needleleaf Evergreen trees
	Needleleaf Deciduous trees
Broadleaf trees	Broadleaf Evergreen trees
	Broadleaf Cold Deciduous trees
	Broadleaf Drought/Dry Deciduous trees
Crops	C3 Crops
	C4 Crops
Grasses	C3 Grasses
	C4 Grasses

Table 2. The location of Fluxnet sites, primary species that exist at these sites, their soil physical characteristics, mean annual values of primary meteorological variables, and years of data availability

Site Name	Harvard forest (US-Ha1)	Morgan Monroe state forest (US-MMS)	Uni. of Mich. Biological station (US-UMB)
Lat, Lon,Elevation	42.53º, -72.17º, 340m	39.32º, -86.41º, 275m	45.55º, -84.71º, 234m
Biome Type	Broadleaf deciduous forest	Broadleaf deciduous forest	Broadleaf deciduous forest
Species	Red Oak (Quercus rubra), Red Maple (Acer rubrum), Hemlock (Tsuga canadensis), White Pine (Pinus strobus)	Maple-beech (Fagus grandifolia), Oak-Hickory	Conifer understory, Aspen (Populus tremuloides), Hemlock (Cicuta), and other northern hardwood trees
Mean annual air T (ºC)	8.2	12.4	7.2
Mean annual precip. (mm)	1189	1083	613
Mean annual SW Radiation (W/m^2)	151	167	154
Mean annual LW Radiation (W/m^2)	263	329	299
Soil depth (m)	2.5	2.5	2.6
% of soil sand (layer 1, 2, 3)	68.5, 66.5, 72.25	21, 22.5, 30.25	71, 72.5, 73.25
% of soil clay (layer 1, 2, 3)	5, 5, 4.25	21, 23, 23.75	7, 7, 7.75
Years for which LAI data are available	1998-2013	1999-2006	1997-2013

Table 3. Simulated and observation-based turbulent energy and carbon fluxes, and LAI at the three Fluxnet sites.

Site name		Harvard forest (US-Ha1)	Morgan Monroe (US-MMS)	Uni. of Mich. (US-UMB)
Land -atmosphere CO_2 fluxes (gC m^{-2} yr^{-1}) and LAI (m^2/m^2)				
Gross primary productivity	Observed	3.9	4.5	3.6
	CLASS-CTEM original	3.6	5.0	3.6
	CLASS-CTEM modified	3.7	5.3	3.7
Ecosystem respiration	Observed	3.3	3.3	2.9
	CLASS-CTEM original	3.6	4.9	3.5
	CLASS-CTEM modified	3.7	5.3	3.7
Net ecosystem productivity	Observed	0.7	1.2	0.7
	CLASS-CTEM original	0.02	0.1	0.0
	CLASS-CTEM modified	0.0	0.0	0.0
Leaf area index	Observed	1.8	3.0	2.8
	CLASS-CTEM original	2.0	3.1	1.9
	CLASS-CTEM modified	1.9	3.0	1.8
Energy fluxes and energy budget (W/m^2)				
Net radiation (R_n)	observed	78.9	89.6	78.1
	CLASS-CTEM original	59.6	89.2	66.8
	CLASS-CTEM modified	59.6	89.6	67.2
Latent heat flux (LE)	observed	34.0	38.3	35.4
	CLASS-CTEM original	38.9	68.6	47.9
	CLASS-CTEM modified	39.4	69.3	48.3
Sensible heat flux (H)	observed	29.3	25.1	29.4
	CLASS-CTEM original	20.7	20.6	18.9
	CLASS-CTEM modified	20.2	20.3	18.9
R_n-LE-H	observed	15.6	26.2	13.3
	CLASS-CTEM original	0	0	0
	CLASS-CTEM modified	0	0	0

List of Figures

Legends also show the mean annual value of the quantity plotted, except for LAI which is averaged over the growing season. Root mean square error (RMSE) and coefficient of determination (R^2) are also shown for simulated values when compared to observation-based estimates.

7 CLASS-CTEM (modified version) simulated values of total (panel a) and non-structural (panel c) carbohydarte pools (Kg C/m^2). Panel (b) shows the reallocation of carbon from non-structural stem and root pools to leaves during leaf onset in spring and panel (d) shows the carbon flux from non-structural to structural pools for leaf, stem and root components (gC/m^2.day) for US-Ha1(Harvard Forest) Fluxnet site. The plots show mean daily values across all years for which the meteorological data were available after the model pools reached equilibrium.

8 CLASS-CTEM (modified version) simulated values of total (panel a) and non-structural (panel c) carbohydarte pools (Kg C/m^2). Panel (b) shows the reallocation of carbon from non-structural stem and root pools to leaves during leaf onset in spring and panel (d) shows the carbon flux from non-structural to structural pools for leaf, stem and root components (g.C/m^2.day) for US-MMS (Morgan Monroe State Forest) Fluxnet site. The plots show mean daily values across all years for which the meteorological data were available after the model pools reached equilibrium.

9 CLASS-CTEM (modified version) simulated values of total (panel a) and non-structural (panel c) carbohydarte pools (Kg C/m^2). Panel (b) shows the reallocation of carbon from non-structural stem and root pools to leaves during leaf onset in spring and panel (d) shows the carbon flux from non-structural to structural pools for leaf, stem and root components (g.C/m^2.day) for US-UMB (University of Michigan Biological Reserve) Fluxnet site. The plots show mean daily values across all years for which the meteorological data were available after the model pools reached equilibrium.

10 Observed and CLASS-CTEM simulated daily net radiation (W/m^2), latent heat flux (W/m^2), and sensible heat flux (W/m^2) for the three Fluxnet sites. Legends also show the mean annual value of the quantity plotted. Root mean square error (RMSE) and coefficient of determination (R^2) are also shown for simulated values when compared to observation-based estimates.

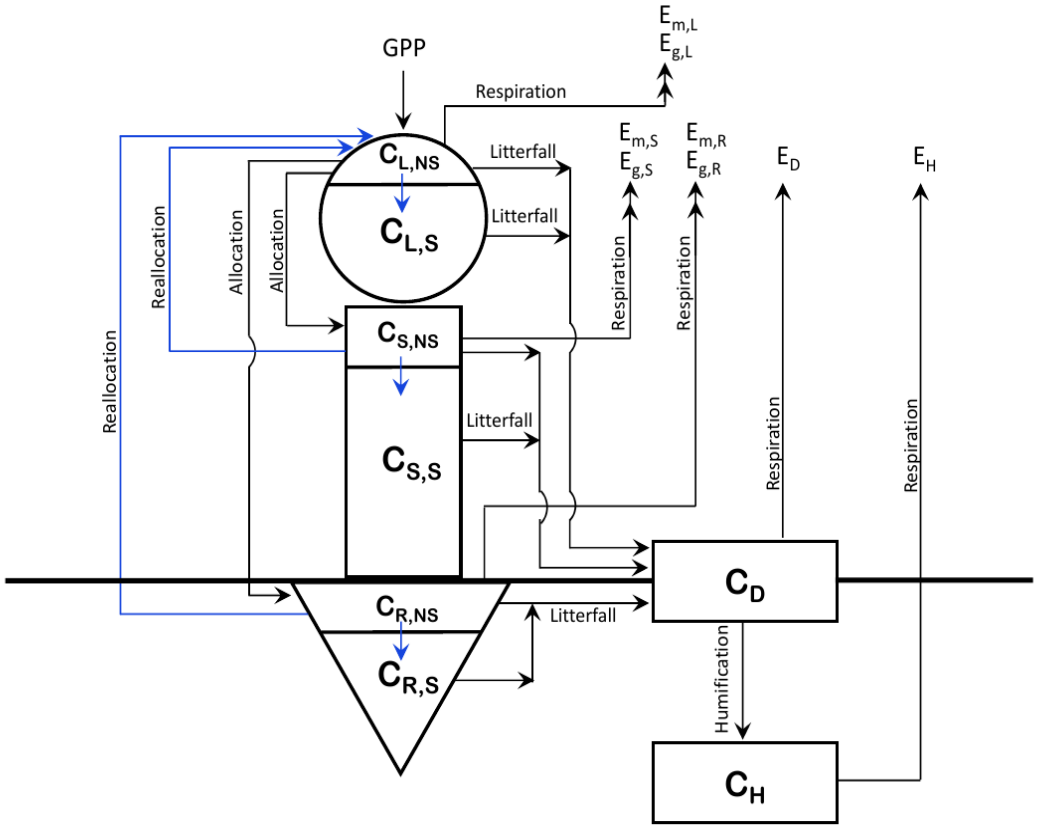

Figure 1: Schematic representation of the CTEM model after addition of non-structural carbohydrate pools. The arrows in blue color show the new non-structural carbohydrate fluxes as shown in Equations 5 and 6.

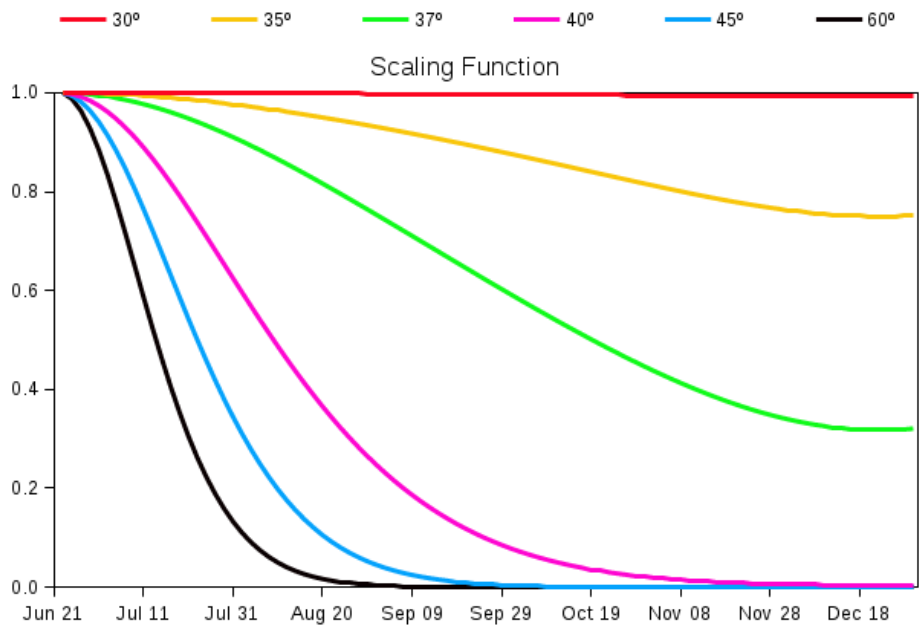

Figure 2: Latitude dependence factor (Γ) (Equation 8) for reducing allocation fraction to leaves after summer solstice.

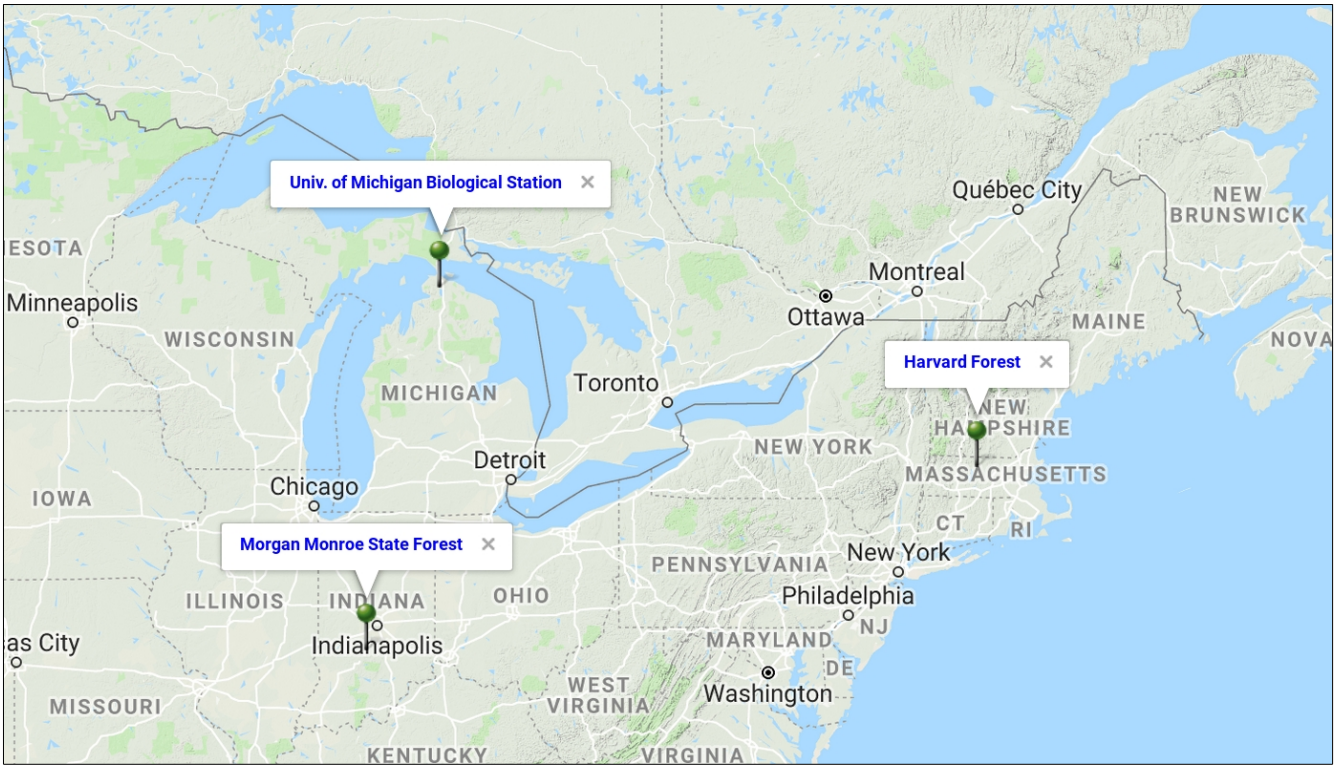

Figure 3: Location of the three Fluxnet sites chosen in this study to evaluate the changes made to the CLASS-CTEM parameterizations aimed to improve leaf phenology. Figure adapted from Google maps.

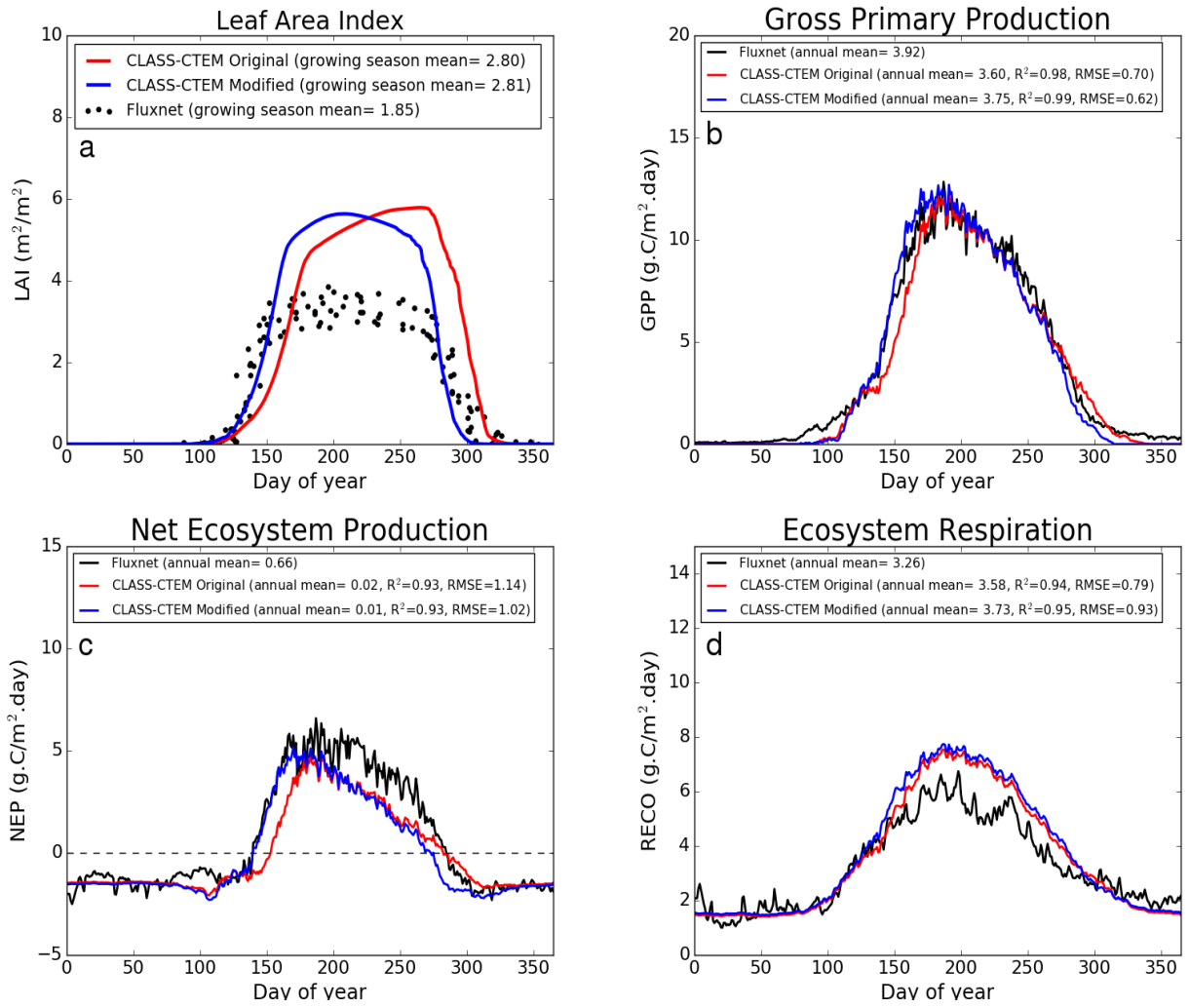

Figure 4: Observed and CLASS-CTEM simulated averaged daily values of a) LAI (m^2/m^2), b) GPP ($g.C/m^2.day$), c) NEP ($g.C/m^2.day$), and d) Ecosystem respiration ($g.C/m^2.day$) for US-Ha1 (Harvard Forest) Fluxnet site across all years were data are present. Legends also show the mean annual value of the quantity plotted, except for LAI which is averaged over the growing season. Root mean square error (RMSE) and coefficient of determination (R^2) are also shown for simulated values when compared to observation-based estimates.

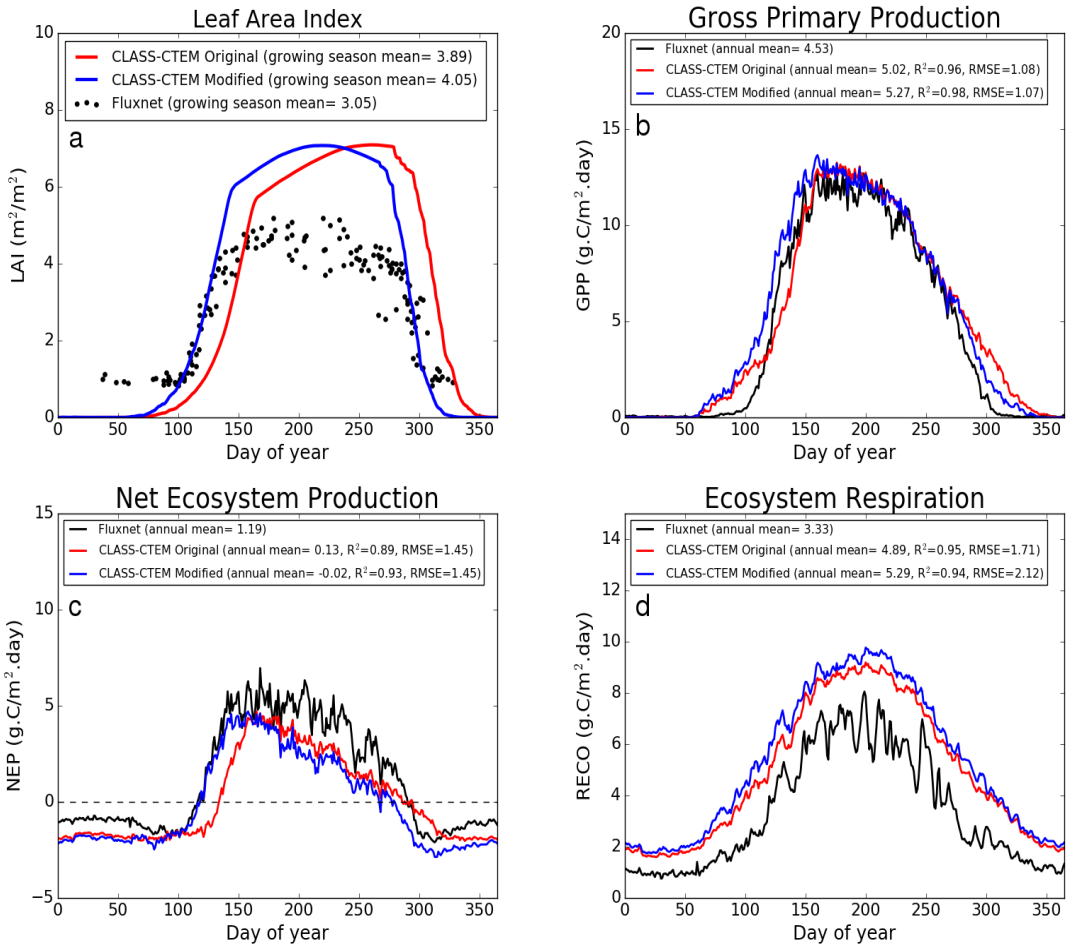

Figure 5: Observed and CLASS-CTEM simulated averaged daily values of a) LAI (m^2/m^2), b) GPP ($g.C/m^2.day$), c) NEP ($g.C/m^2.day$), and d) Ecosystem respiration ($g.C/m^2.day$) for US-MMS (Morgan Monroe State Forest) Fluxnet site across all years were data are present. Legends also show the mean annual value of the quantity plotted, except for LAI which is averaged over the growing season. Root mean square error (RMSE) and coefficient of determination (R^2) are also shown for simulated values when compared to observation-based estimates.

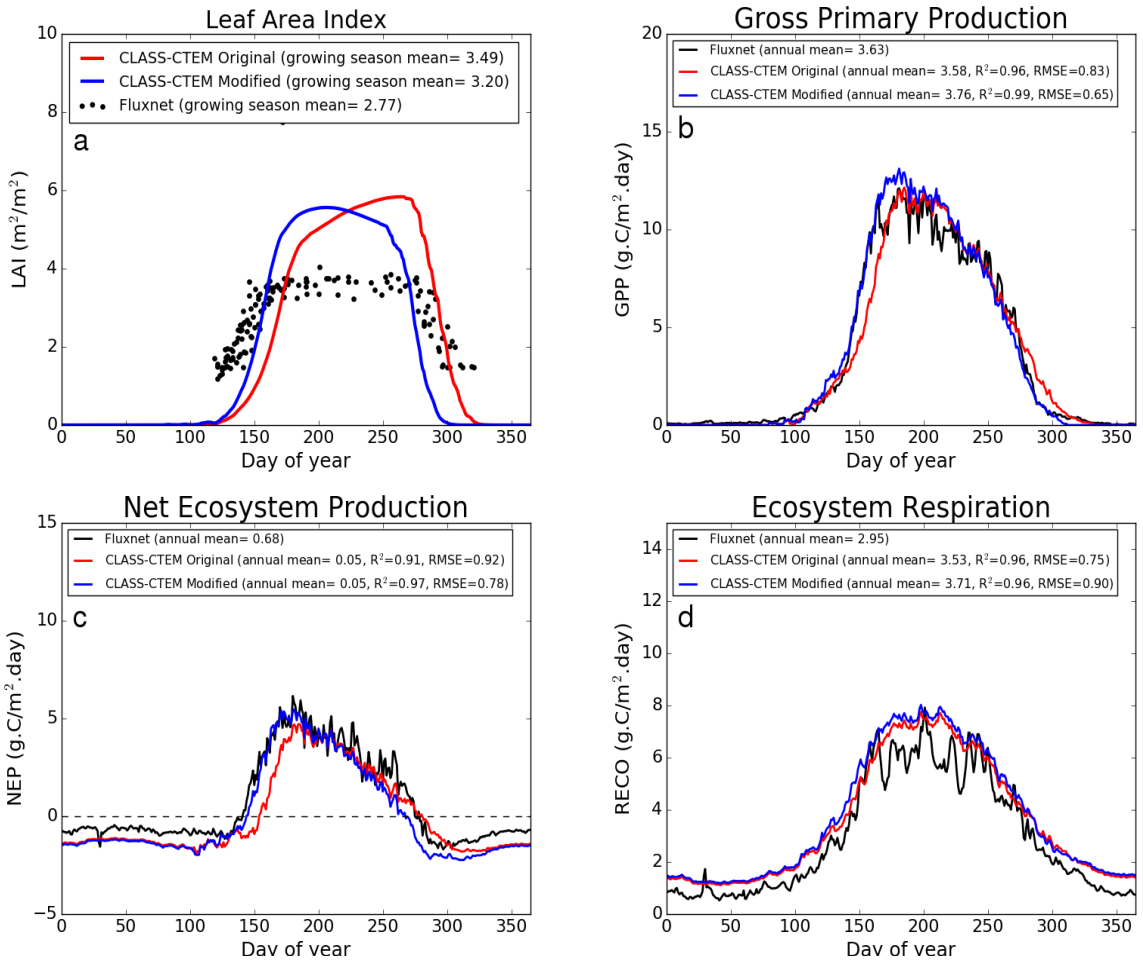

Figure 6: Observed and CLASS-CTEM simulated averaged daily values of a) LAI (m^2/m^2), b) GPP ($g.C/m^2.day$), c) NEP ($g.C/m^2.day$), and d) Ecosystem respiration ($g.C/m^2.day$) for US-UMB (University of Michigan Biological Reserve) Fluxnet site across all years were data are present. Legends also show the mean annual value of the quantity plotted, except for LAI which is averaged over the growing season. Root mean square error (RMSE) and coefficient of determination (R^2) are also shown for simulated values when compared to observation-based estimates.

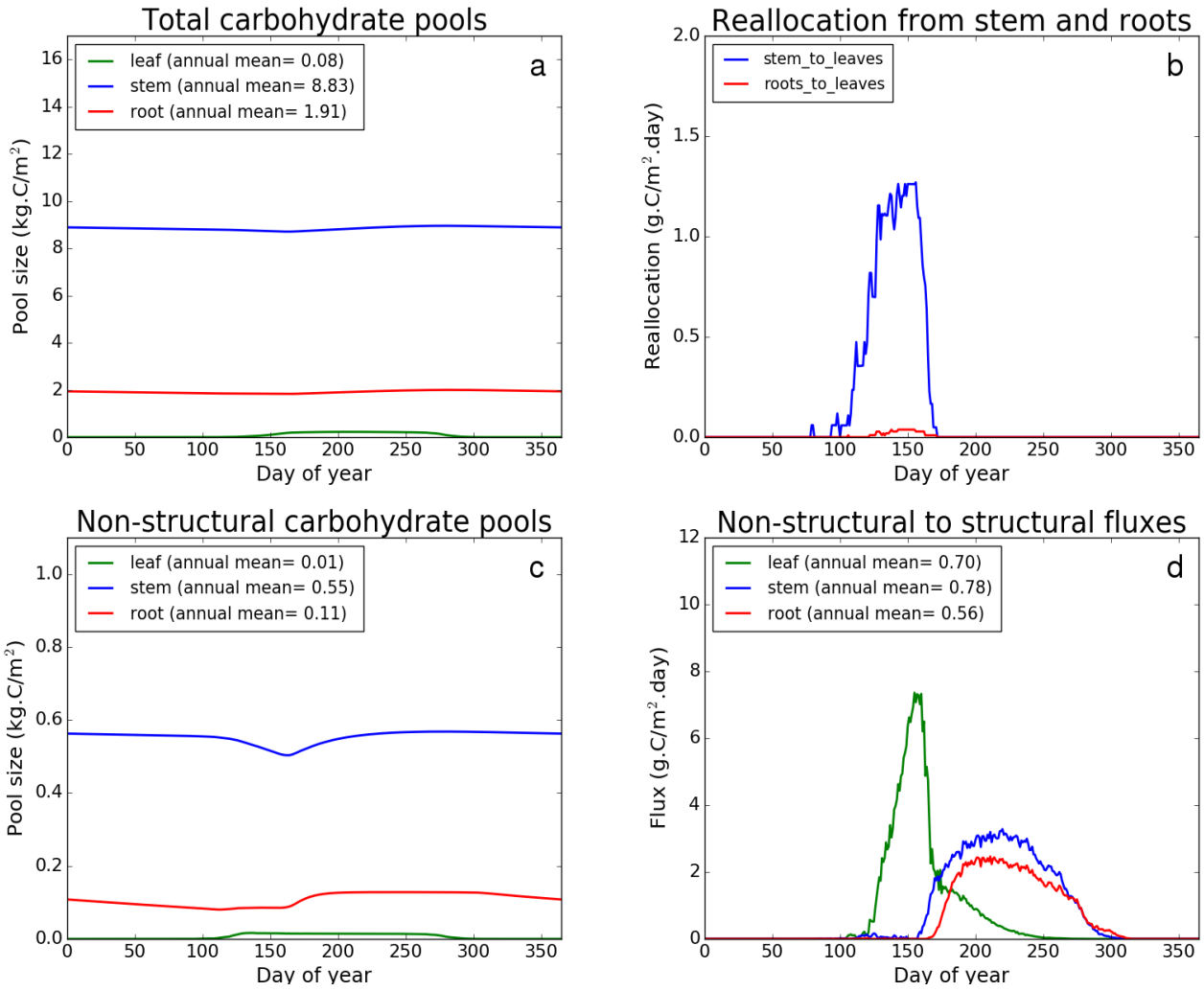

Figure 7: CLASS-CTEM (modified version) simulated values of total (panel a) and non-structural (panel c) carbohydarte pools (Kg C/m^2). Panel (b) shows the reallocation of carbon from non-structural stem and root pools to leaves during leaf onset in spring and panel (d) shows the carbon flux from non-structural to structural pools for leaf, stem and root components (gC/m^2.day) for US-Ha1(Harvard Forest) Fluxnet site. The plots show mean daily values across all years for which the meteorological data were available after the model pools reached equilibrium.

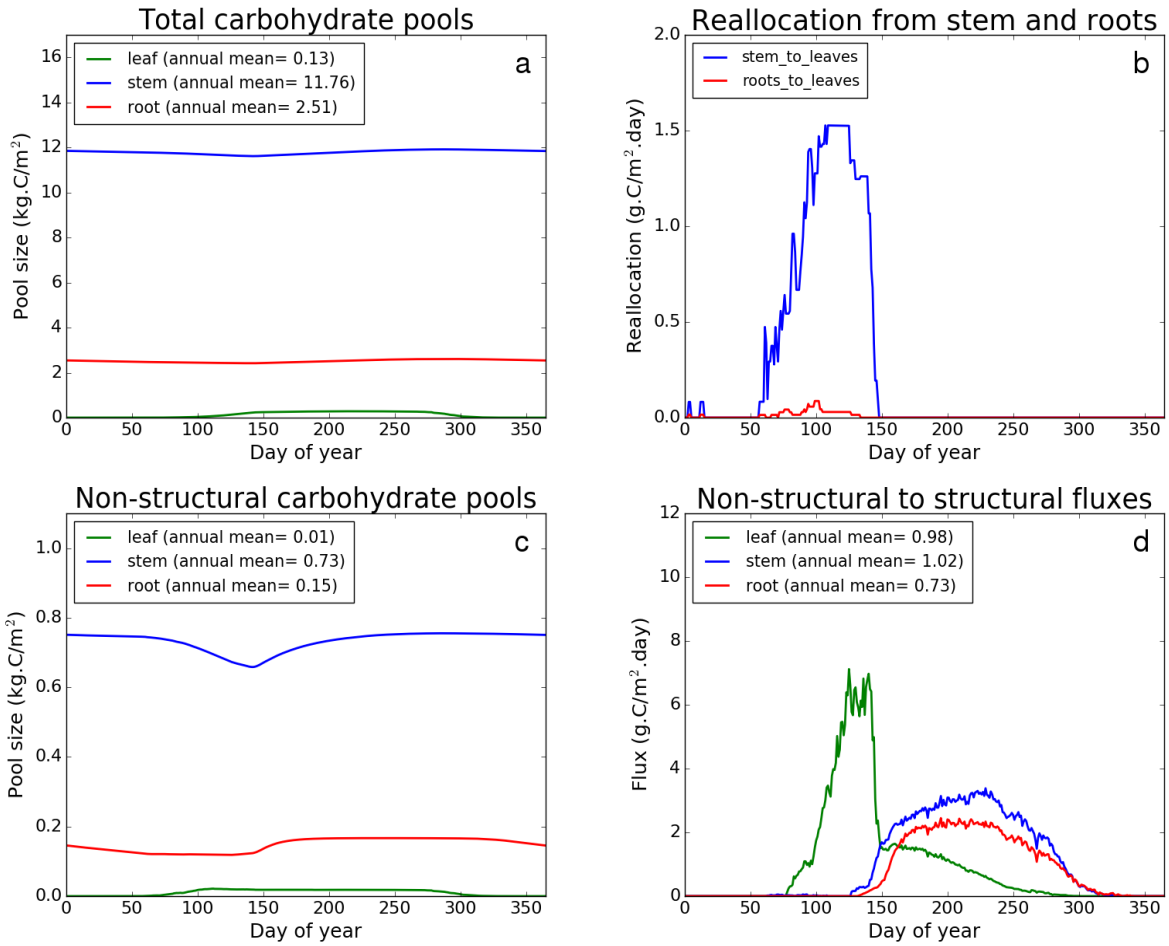

Figure 8: CLASS-CTEM (modified version) simulated values of total (panel a) and non-structural (panel c) carbohydarte pools (Kg C/m^2). Panel (b) shows the reallocation of carbon from non-structural stem and root pools to leaves during leaf onset in spring and panel (d) shows the carbon flux from non-structural to structural pools for leaf, stem and root components (g.C/m^2.day) for US-MMS (Morgan Monroe State Forest) Fluxnet site. The plots show mean daily values across all years for which the meteorological data were available after the model pools reached equilibrium.

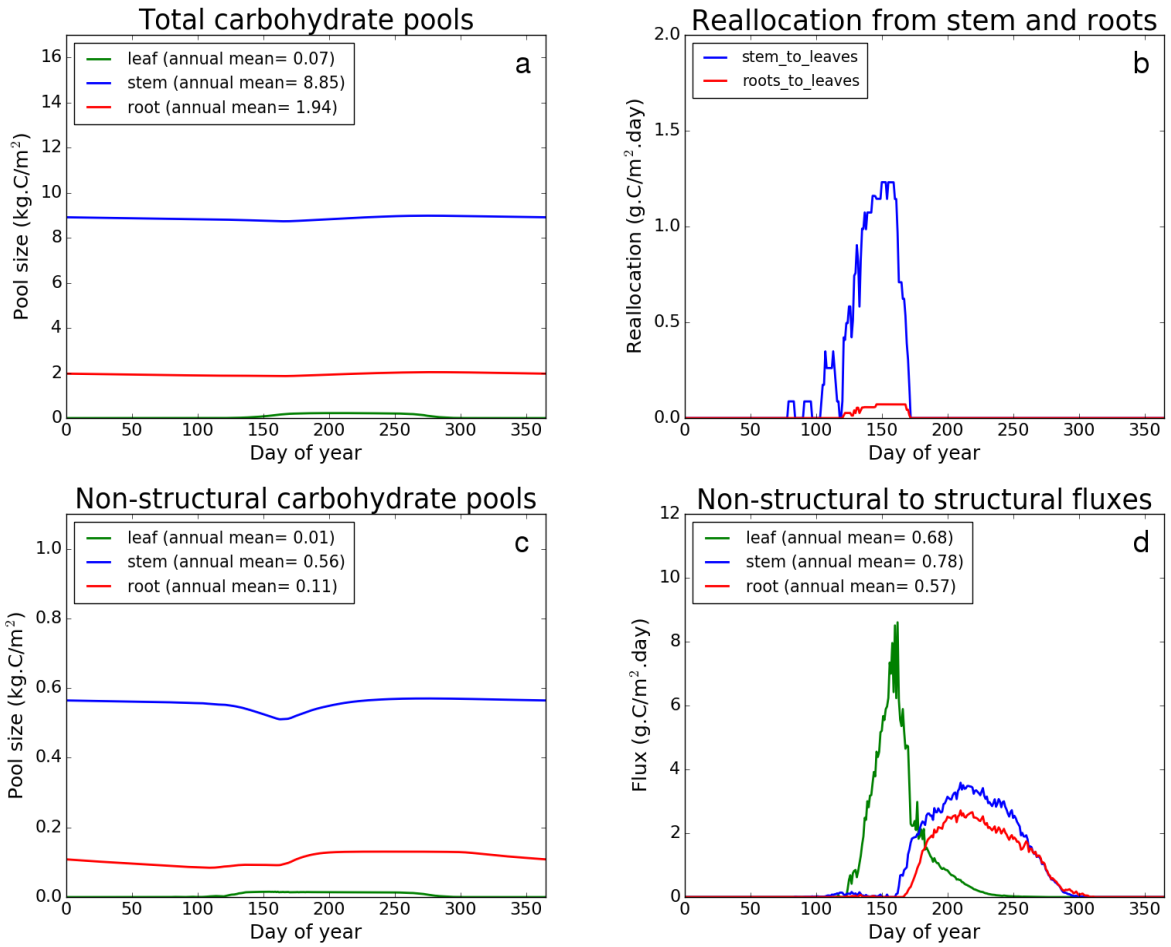

Figure 9: CLASS-CTEM (modified version) simulated values of total (panel a) and non-structural (panel c) carbohydarte pools (Kg C/m^2). Panel (b) shows the reallocation of carbon from non-structural stem and root pools to leaves during leaf onset in spring and panel (d) shows the carbon flux from non-structural to structural pools for leaf, stem and root components (g.C/m^2.day) for US-UMB (University of Michigan Biological Reserve) Fluxnet site. The plots show mean daily values across all years for which the meteorological data were available after the model pools reached equilibrium.

Harvard Forest Morgan Monroe University of Michigan

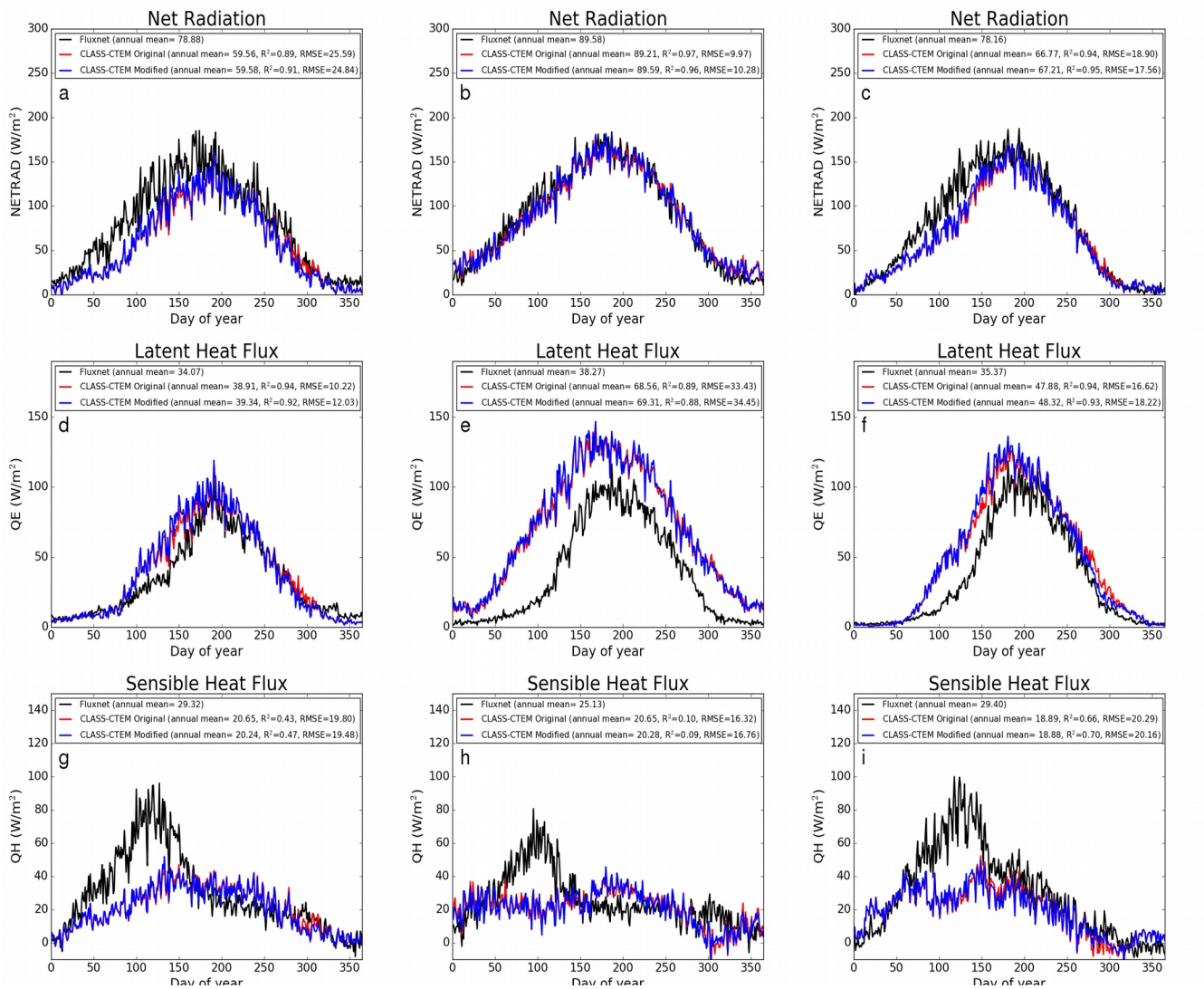

Figure 10: Observed and CLASS-CTEM simulated daily net radiation (W/m^2), latent heat flux (W/m^2), and sensible heat flux (W/m^2) for the three Fluxnet sites. Legends also show the mean annual value of the quantity plotted. Root mean square error (RMSE) and coefficient of determination (R^2) are also shown for simulated values when compared to observation-based estimates.